INTERNATIONAL JOURNAL FOR NUMERICAL METHODS IN ENGINEERING, VOL. 36, 3097–3130 (1993)

A BOUNDARY ELEMENT FORMULATION BASED ON THE THREE-DIMENSIONAL ELASTOSTATIC FUNDAMENTAL SOLUTION FOR THE INFINITE LAYER: PART I—THEORETICAL AND NUMERICAL DEVELOPMENT

F. G. BENITEZ*

Department of Mechanical Engineering, University of Sevilla, Avda. Reina Mercedes, Sevilla-41012, Spain

L. LU† AND A. J. ROSAKIS‡

Division of Engineering and Applied Sciences, California Institute of Technology, 105-50, Pasadena, CA 91125, U.S.A.

SUMMARY

This work presents a specialization of the integral identities used in the boundary element method. This modification is especially tailored to deal with three-dimensional elastostatic problems involving geometries which contain two parallel planar surfaces (e.g. three-dimensional plate problems). The formulation makes use of the three-dimensional fundamental solution for a point load acting in the interior of an infinite layer of uniform thickness (obtained by Benitez and Rosakis[8,9]).

It is shown that this procedure is especially suited for the analysis of three-dimensional problems involving cavities in plate structures. In such problems it is demonstrated that, in addition to the cavity surfaces, only the lateral surfaces of the structure need to be discretized, with no discretization required on the traction-free parallel surfaces.

1. INTRODUCTION

The boundary element method (BEM) has become a powerful alternative numerical technique to the finite element method (FEM). Both numerical methods have been widely used to study elastostatic, elastoplastic, transient and dynamic problems. In some problems, the BEM has shown a series of advantages over the FEM. The fact that the discretization is only performed on the surface of the solid under study implies a reduction of the dimensionality of the problem by one and, therefore, it is easier to modify the discretization mesh. Once the boundary solution has been numerically obtained, interior values may easily be determined. This feature is particularly advantageous for modelling regions with high stress gradients with great accuracy and efficiency, making this technique an appealing tool for the numerical solution of problems in linear fracture mechanics. In addition, the BEM is specially well suited to elastic problems involving infinite regions. Finally, since the formulation is based on fundamental solutions that satisfy the governing differential equations, approximation of the variables is required only on the boundary. This implies, in most cases, better accuracy.

---

* Professor
† Graduate Student
‡ Associate Professor

0029–5981/93/183097–34$22.00

Received 21 April 1992
Revised 18 February 1993

The advantages over FEM are more clearly manifested when the ratio of surface to volume in the solid is low. In particular, this quotient is high for three-dimensional plate structures; therefore, in order to retain the boundary element method capabilities, it is desirable to use the three-dimensional fundamental solution for an infinite layer. By using this solution the need for discretization of the two end parallel surfaces disappears, as long as they are traction-free.

In a number of studies, various boundary integral formulations have been shown to be useful for particular classes of boundary-value problems. The main difference among them focusses on the use of diverse Green's functions fundamental solutions, which are more appropriate for dealing with the geometry of the problem considered. Thus, for generic two- and three-dimensional elastostatic problems, Kelvin's fundamental solution derived in 1848[1] of a concentrated load in an infinite medium has been widely used.[2,3] This solution is available in close-form expressions of relative simplicity. Also, for problems involving a single free surface the solution presented by Melan,[4] for the stress distribution due to a point load applied within an infinite two-dimensional semi-space, or the one given by Mindlin,[5] for the three-dimensional case, are of great interest. These latter fundamental solutions have been applied to the boundary element technique by diverse investigators.[6,7]

The work presented in this paper reports on a specialization of the integral identities used in the boundary element method appropriate for the numerical solution of elastostatic three-dimensional problems involving plate regions. The formulation makes use of the fundamental solution of a concentrated load in an infinite three-dimensional elastic layer of uniform thickness, which was obtained by Benitez and Rosakis.[8,9]

In the first part of this paper, the nature of this fundamental solution and its use into a boundary element scheme is described. In the second part, the numerical implementation of the technique is tackled.

2. BASIC MATHEMATICAL CONCEPTS

Let E_3 denote the three-dimensional Euclidean space. Let $\mathbf{x} = (x_1, x_2, x_3)$ be the position vector of a point in E_3. The symbols $B_\eta(\mathbf{x})$ and $\partial B_\eta(\mathbf{x})$ denote an open sphere and its surface, respectively. The sphere is centred at $\mathbf{x}$ with a radius η.

Let $\mathscr{R}$ be an arbitrary regular region in the sense of Kellogg,[10] in E_3. The boundary, interior and closure of $\mathscr{R}$ are $\partial\mathscr{R}, \mathring{\mathscr{R}}$ and $\bar{\mathscr{R}}$, respectively. In the case of $\mathbf{x} \in \mathscr{R}$, $\mathscr{R} - \{\mathbf{x}\}$ represents the set obtained by the deletion of point $\mathbf{x}$ from $\mathscr{R}$.

Standard indicial notation will be used in connection with the Cartesian components of tensors of any order. Subscripts preceded by a comma indicate partial differentiation with respect to the corresponding Cartesian co-ordinates. For functions having more than one vector variable, the differentiation mentioned above will be understood to be performed on the first vector variable; thus

$$\underbrace{f_{,ij\cdots k}}_{n \text{ indices}}(\mathbf{x}, \mathbf{y}) = \frac{\partial^n f(\mathbf{x}, \mathbf{y})}{\partial x_i \partial x_j \cdots \partial x_k} \tag{1}$$

We write $g(\mathbf{x}) \in \mathscr{C}(\mathscr{R})$ if g is defined and is continuous on a region $\mathscr{R} \in E_3$. Moreover, if m is a positive integer, we write $g \in \mathscr{C}^m(\mathscr{R})$ when $g \in \mathscr{R}$ and its partial derivatives of order up to and including m are defined as well as continuous on $\mathring{\mathscr{R}}$ and they coincide with functions continuous on $\mathring{\mathscr{R}}$.

We write

$$\mathscr{S} = [\mathbf{u}, \boldsymbol{\sigma}] \in \mathscr{E}_s(E, \nu, \mathbf{f}; \mathscr{R}) \tag{2}$$

and say that the ordered array $\mathscr{S} = [\mathbf{u}, \boldsymbol{\sigma}]$ of displacement and stress fields is an *elastostatic state* on $\mathscr{R}$ corresponding to the body force density $\mathbf{f}$, provided

(a) $\mathbf{u} \in \mathscr{C}^1(\mathring{\mathscr{R}}) \cap \mathscr{C}(\mathscr{R})$, $\boldsymbol{\sigma} \in \mathscr{C}^1(\mathring{\mathscr{R}}) \cap \mathscr{C}(\mathscr{R})$, $\mathbf{f} \in \mathscr{C}(\mathscr{R})$, where E (Young's modulus) and ν (Poisson's ratio) are constants with $E > 0$, $-1 < \nu < \frac{1}{2}$.

(b) $\mathbf{u}, \boldsymbol{\sigma}, \mathbf{f}, E$ and ν satisfy the following equations on $\mathring{\mathscr{R}}$:

$$\begin{gathered} \nabla \cdot \boldsymbol{\sigma} + \mathbf{f} = \mathbf{0}, \quad \boldsymbol{\sigma} = \boldsymbol{\sigma}^{\mathrm{T}} \\ \boldsymbol{\sigma} = \frac{\nu E}{(1+\nu)(1-2\nu)} [\nabla \cdot \mathbf{u}] \mathbf{I} + \frac{E}{2(1+\nu)} [\nabla \mathbf{u} + \nabla^{\mathrm{T}} \mathbf{u}] \end{gathered} \tag{3}$$

Furthermore, if $\mathscr{S} = [\mathbf{u}, \boldsymbol{\sigma}]$ is an elastostatic state on $\mathscr{R}$ and Σ is a regular surface with the unit normal $\mathbf{n}$,we call $\mathbf{t}$ the traction vector of $\mathscr{S}$ on Σ if

$$t_i = \sigma_{ij} n_j \quad \text{on } \overset{*}{\Sigma} \tag{4}$$

where $\overset{*}{\Sigma}$ is the subset of all points of Σ at which a normal is defined.

Further, let $\mathscr{S}' = [\mathbf{u}', \boldsymbol{\sigma}'] \in \mathscr{E}_s(E, \nu, \mathbf{f}'; \mathscr{R})$ and $\mathscr{S}'' = [\mathbf{u}'', \boldsymbol{\sigma}''] \in \mathscr{E}_s(E, \nu, \mathbf{f}''; \mathscr{R})$. Furthermore let $\mathbf{t}' = \boldsymbol{\sigma}' \cdot \mathbf{n}$, $\mathbf{t}'' = \boldsymbol{\sigma}'' \cdot \mathbf{n}$ on $\partial\mathscr{R}$. Then Betti's reciprocal theorem in elastostatics holds.[11]

$$\int_{\partial\mathscr{R}} \mathbf{t}'(\mathbf{x}) \cdot \mathbf{u}''(\mathbf{x}) \, \mathrm{d}A + \int_{\mathscr{R}} \mathbf{f}'(\mathbf{x}) \cdot \mathbf{u}''(\mathbf{x}) \, \mathrm{d}V = \int_{\partial\mathscr{R}} \mathbf{t}''(\mathbf{x}) \cdot \mathbf{u}'(\mathbf{x}) \, \mathrm{d}A + \int_{\mathscr{R}} \mathbf{f}''(\mathbf{x}) \cdot \mathbf{u}'(\mathbf{x}) \, \mathrm{d}V \tag{5}$$

3. THREE-DIMENSIONAL ELASTOSTATIC FUNDAMENTAL SOLUTION FOR THE INFINITE LAYER

3.1. Nature of the solution

The following development, of the necessary theoretical background regarding the problem of a concentrated load applied at an interior or surface point of a homogeneous, isotropic, linear elastic body occupying an infinite elastic layer of uniform thickness h, is based on previous progress by Benitez and Rosakis.[12] Several important properties of the solution and the associated doublet states are also summarized.

Consider now a proper orthogonal Cartesian frame, $\mathbf{X} = \{0; \mathbf{e}_1, \mathbf{e}_2, \mathbf{e}_3\}$. Define the infinite region $\mathscr{P} \subset E_3$ as follows:

$$\begin{gathered} \mathscr{P} = \{\mathbf{x} | \mathbf{x} \in E_3, \, 0 \leqslant \mathbf{x} \cdot \mathbf{e}_3 \leqslant h\} \\ \text{and let } \partial\mathscr{P} = \partial\mathscr{P}_1 \cup \partial\mathscr{P}_2, \text{ where} \\ \partial\mathscr{P}_1 = \{\mathbf{x} | \mathbf{x} \in E_3, \, \mathbf{x} \cdot \mathbf{e}_3 = 0\}, \quad \partial\mathscr{P}_2 = \{\mathbf{x} | \mathbf{x} \in E_3, \, \mathbf{x} \cdot \mathbf{e}_3 = h\} \end{gathered} \tag{6}$$

Let $\boldsymbol{\xi} \in \mathscr{P}$ be the point of application of a concentrated load $\mathbf{I}$. Caution should be exercised in the meaning attached to concentrated load at a point as discussed by Turteltaub and Sternberg.[13] Here we adopt the so-called direct formulation of the concentrated load problem. The problem can be formulated as follows.

We seek an ordered array $\mathscr{S}(\mathbf{x}, \xi, \mathbf{l}) = [\mathbf{u}(\mathbf{x}, \xi, \mathbf{l}); (\boldsymbol{\sigma}, \xi, \mathbf{l})]$ of displacement and stress fields with the following properties:

$$\mathscr{S} = [\mathbf{u}, \boldsymbol{\sigma}] \in \mathscr{E}_s(E, \nu, \mathbf{0}; \mathscr{P} - \{\xi\}) \tag{7a}$$

$$\mathbf{t}(\mathbf{x}, \xi) = \boldsymbol{\sigma}(\mathbf{x}, \xi) \cdot \mathbf{n} = \mathbf{0}, \quad \begin{cases} \forall \mathbf{x} \in \partial\mathscr{P} & \text{for } \xi \in \mathring{\mathscr{P}} \\ \forall \mathbf{x} \in \partial\mathscr{P} - \{\xi\} & \text{for } \xi \in \partial\mathscr{P} \end{cases} \tag{7b}$$

$$\lim_{\eta \to 0} \int_{\mathscr{P} \cap \partial B_\eta(\xi)} \mathbf{t}(\mathbf{x}, \xi) \mathrm{d}A_x = \mathbf{1}, \quad \lim_{\eta \to 0} \int_{\mathscr{P} \cap \partial B_\eta(\xi)} (\mathbf{x} - \xi) \Lambda \mathbf{t}(\mathbf{x}, \xi) \, \mathrm{d}A_x = \mathbf{0}, \quad \text{for } \xi \in \mathscr{P} \tag{7c}$$

$$\mathbf{u}(\mathbf{x}) = \mathscr{O}(|\mathbf{x} - \xi|^{-1}), \quad \boldsymbol{\sigma}(\mathbf{x}) = \mathscr{O}(|\mathbf{x} - \xi|^{-2}) \quad \text{as } \mathbf{x} \to \xi \tag{7d}$$

where $\mathbf{t}$ in (7c) is the traction vector on the side of $\mathscr{P} \cap \partial B_\eta(\xi)$ that faces ξ.

Let $\mathscr{S}(\mathbf{x}, \xi, \mathbf{l})$ denote the elastostatic state satisfying (7a)–(7d). Let $\mathbf{X} = \{0; \mathbf{e}_1, \mathbf{e}_2, \mathbf{e}_3\}$ be a proper orthogonal frame. We define

$$\mathscr{S}^k(\mathbf{x}, \xi) = \mathscr{S}(\mathbf{x}, \xi, \mathbf{e}_k), \quad (k = 1, 2, 3) \tag{8}$$

as the triplet of normal states whose displacement and stress fields are given by the solution appropriate to concentrated *unit loads* and equal to $\mathbf{e}_k$. We also introduce the notation

$$\mathscr{S}^k(\mathbf{x}, \xi) = [\mathbf{u}^k(\mathbf{x}, \xi); \boldsymbol{\sigma}^k(\mathbf{x}, \xi)] \equiv [\mathbf{u}^k(\mathbf{x}, \xi, \mathbf{e}_k); \boldsymbol{\sigma}^k(\mathbf{x}, \xi, \mathbf{e}_k)] \tag{9}$$

Definitions (8) and (9) and the principle of superposition for linear elasticity imply

$$\mathscr{S}(\mathbf{x}, \xi, \mathbf{l}) = \mathscr{S}^k(\mathbf{x}, \xi)\mathbf{l}_k, \quad \forall \mathbf{x} \in \mathscr{P} - \{\xi\} \tag{10}$$

or equivalently from (9)

and

$$\begin{aligned} \mathbf{u}(\mathbf{x}, \xi, \mathbf{l}) &= (u_i^k(\mathbf{x}, \xi) \cdot \mathbf{l}_k) \cdot \mathbf{e}_i \\ \boldsymbol{\sigma}(\mathbf{x}, \xi, \mathbf{l}) &= (\sigma_{ij}^k(\mathbf{x}, \xi) \cdot \mathbf{l}_k) \cdot \mathbf{e}_i \Lambda \mathbf{e}_j \end{aligned} \tag{11}$$

where $u_i^k(\mathbf{x}, \xi)$ and $\sigma_{ij}^k(\mathbf{x}, \xi)$ are the Cartesian components in $\mathbf{X}$ of $\mathbf{u}^k(\mathbf{x}, \xi)$ and $\boldsymbol{\sigma}^k(\mathbf{x}, \xi)$, respectively.

It should also be noted that the state $\mathscr{S}(\mathbf{x}, \xi, \mathbf{l})$ also satisfies the following identity known as the *translation identity*, i.e.,

$$\mathscr{S}(\mathbf{x}, \mathbf{a} + \xi, \mathbf{l}) = \mathscr{S}(\mathbf{x} - \xi, \mathbf{a}, \mathbf{l}) \tag{12}$$

for all $\mathbf{x} \in \mathscr{P} - \{\xi + \mathbf{a}\}$ and for all vectors $\mathbf{a}, \xi \in \mathscr{P}$. If, in particular, for $\mathbf{a} = \mathbf{0}$ and $\mathbf{l} = \mathbf{e}_k$, we have

$$\mathscr{S}^k(\mathbf{x}, \xi) = \mathscr{S}^k(\mathbf{x} - \xi, \mathbf{0}), \quad \forall \mathbf{x} \in \mathscr{P} - \{\xi\} \tag{13}$$

Expressions for $u_i^k(\mathbf{x}, \xi)$ and $\sigma_{ij}^k(\mathbf{x}, \xi)$ are provided by Benitez and Rosakis,[8,9] where it is shown that the associated state $\mathscr{S}^k(\mathbf{x}, \xi)$ indeed satisfies the requirements (7a)–(7d). The displacement and stress fields are given with respect to a Cartesian co-ordinate frame $\mathbf{X} = \{0; \mathbf{e}_1, \mathbf{e}_2, \mathbf{e}_3\}$ such that the origin 0 lies on one of the two parallel traction-free surfaces of the infinite layer ($0 \in \partial\mathscr{P}_1$), and such that $\mathbf{e}_3 = -\mathbf{n}$, when $\mathbf{n}$ is the outward normal to $\partial\mathscr{P}_1$ (see Figure 1). In addition, the results by Benitez and Rosakis[8,9] are obtained for $\xi = H\mathbf{e}_3$, $0 \leqslant H \leqslant h$, where h is the layer thickness. Nevertheless, in view of properties (10)–(13), this solution is enough to define $\mathscr{S}(\mathbf{x}, \xi, \mathbf{l})$ completely for any vectors ξ and $\mathbf{l}$.

Although the complete set of expressions for $\mathscr{S}^k(\mathbf{x}, \xi)$, $k = 1, 2, 3$ and $\xi = H\mathbf{e}_3$ are given by Benitez and Rosakis,[9] for the sake of completeness they are stated in Appendix I with respect to a Cartesian co-ordinate frame $\mathbf{X} = \{0; \mathbf{e}_1, \mathbf{e}_2, \mathbf{e}_3\}$ such that $0 \in \partial\mathscr{P}_1$, and $\mathbf{e}_3 = -\mathbf{n}$, where $\partial\mathscr{P}_1 = \{\mathbf{x} | \mathbf{x} \in \mathscr{P}, \mathbf{x} \cdot \mathbf{e}_3 = 0\}$, is the lower traction-free surface of the layer, and $\mathbf{n}$ is the outward normal to $\partial\mathscr{P}_1$.

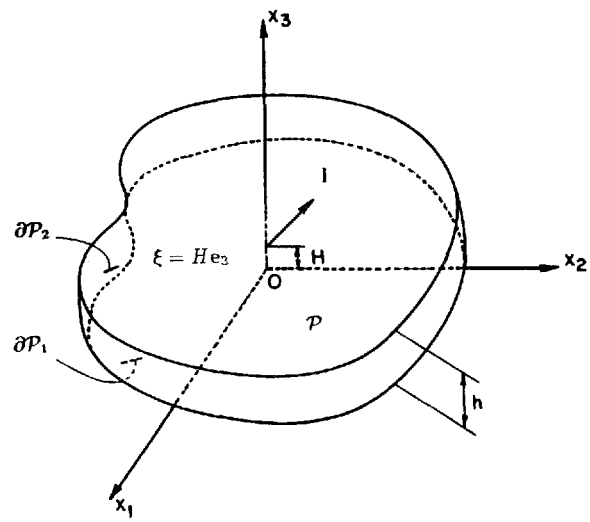

Figure 1. Schematic of a concentrated load l acting at the interior of an infinite elastic layer of uniform thickness h, occupying the infinite region $\mathscr{P}$

As discussed in detail by Benitez and Rosakis,[9] the solution for the concentrated load in an infinite elastic layer of uniform thickness satisfies requirements (7a)–(7d) for $\mathbf{l} = \mathbf{e}_k$, and can thus serve as a fundamental solution to be used in the boundary integral formulation described in the following sections. In particular, it has been shown that the present solution reduces, for $\xi \in \mathring{\mathscr{P}}$, to the well-known Kelvin state (point load in an elastic body occupying E_3) in the limit as $\mathbf{x} \to \xi$. This property is important in the following discussions.

3.2. *Doublet states for the three-dimensional layer*

Let $\mathbf{X} = \{0; \mathbf{e}_1, \mathbf{e}_2, \mathbf{e}_3\}$ be a proper orthogonal frame and let $\mathscr{S}^k(\mathbf{x}, \xi) = \mathscr{S}(\mathbf{x}, \xi, \mathbf{e}_k)$. Then the nine states $\mathscr{S}^{kl}(\mathbf{x}, \xi)$ defined by

$$\mathscr{S}^{kl}(\mathbf{x}, \xi) = \frac{\partial}{\partial x_l} \mathscr{S}^k(\mathbf{x}, \xi) = \mathscr{S}^k_{,l}(\mathbf{x}, \xi), \quad \forall \mathbf{x} \in \mathscr{P} - \{\xi\} \tag{14}$$

are said to be states corresponding to a force doublet applied at ξ(and to E, ν = constant). The above are also elastostatic states.

We also write

$$\mathscr{S}^{kl}(\mathbf{x}, \xi) = [\mathbf{u}^k_{,l}(\mathbf{x}, \xi); \boldsymbol{\sigma}^k_{,l}(\mathbf{x}, \xi)] = [\mathbf{u}^{kl}(\mathbf{x}, \xi); \boldsymbol{\sigma}^{kl}(\mathbf{x}, \xi)], \quad \forall \mathbf{x} \in \mathscr{P} - \{\xi\} \tag{15}$$

and note that the following identity holds:

$$\mathscr{S}^{kl}(\mathbf{x}, \xi) = \mathscr{S}^{kl}(\mathbf{x} - \xi, \mathbf{0}), \quad \forall \mathbf{x} \in \mathscr{P} - \{\xi\} \tag{16}$$

The Cartesian components of displacement and stress belonging to $\mathscr{S}^{kl}(\mathbf{x}, \xi)$ may be derived from the results in Appendix I by means of (15).

Analogous to the preceding layer state discussed in Section 3.1, the layer-doublet states $\mathscr{S}^{kl}(\mathbf{x},\xi)$ have the following properties:

$$\mathscr{S}^{kl}(\mathbf{x},\xi)\in\mathscr{E}_s(E,\nu,\mathbf{0};\mathscr{P}-\{\xi\}) \tag{17a}$$

$$\mathbf{t}^{kl}(\mathbf{x},\xi)=\boldsymbol{\sigma}^{kl}(\mathbf{x},\xi)\cdot\mathbf{n}(\mathbf{x})=\mathbf{0},\quad \forall\begin{cases}\forall\,\mathbf{x}\in\partial\mathscr{P} & \text{if } \xi\in\mathring{\mathscr{P}}\\ \forall\,\mathbf{x}\in\partial\mathscr{P}-\{\xi\} & \text{if } \xi\in\partial\mathscr{P}\end{cases} \tag{17b}$$

$$\lim_{\eta\to 0}\int_{\mathscr{P}\cap\partial B_\eta(\xi)}\mathbf{t}^{kl}(\mathbf{x},\xi)\,\mathrm{d}A_x=\mathbf{0},\quad \lim_{\eta\to 0}\int_{\mathscr{P}\cap\partial B_\eta(\xi)}(\mathbf{x}-\xi)\Lambda\mathbf{t}^{kl}(\mathbf{x},\xi)\,\mathrm{d}A_x=\varepsilon_{klm}\mathbf{e}_m \tag{17c}$$

$$\mathbf{u}^{kl}(\mathbf{x},\xi)=\mathcal{O}(|\mathbf{x}-\xi|^{-2}),\quad \boldsymbol{\sigma}^{kl}(\mathbf{x},\xi)=\mathcal{O}(|\mathbf{x}-\xi|^{-3})\quad \text{as } \mathbf{x}\to\xi \tag{17d}$$

where ε_{klm} is the permutation symbol.

Proof of the above follows by making use of the results in Appendix 1 and the properties of the three-dimensional layer states $\mathscr{S}^k(\mathbf{x},\xi)$. In particular, (17d) follows from the fact that $\mathscr{S}^k(\mathbf{x},\xi)$ for the layer reduces to the well-known Kelvin states as $\mathbf{x}\to\xi$. As a result, $\mathscr{S}^{kl}(\mathbf{x},\xi)$, the doublet states for the layer problem, also reduce to the doublet states for Kelvin's problem as $\mathbf{x}\to\xi$.

4. ELASTOSTATIC BOUNDARY INTEGRAL EQUATION FORMULATION

The generalization of Betti's reciprocal theorem involving singular states is due to Somigliana and has been rigorously proved by Turteltaub and Sternberg.[13]

Let $\mathscr{R}$ be a regular region and let $\xi\in\mathring{\mathscr{R}}$. Furthermore, let $\mathscr{S}$ and $\mathscr{S}'$ be two states with the following properties:

State $\mathscr{S}'$(singular state):

$$\mathscr{S}'=[\mathbf{u}',\boldsymbol{\sigma}']\in\mathscr{E}_s(E,\nu,\mathbf{f}';\bar{\mathscr{R}}-\{\xi\}),\quad \mathbf{f}'\in\mathscr{C}(\bar{\mathscr{R}}), \tag{18a}$$

$$\mathbf{u}'(\mathbf{x},\xi)=\mathcal{O}(|\mathbf{x}-\xi|^{-1}),\quad \boldsymbol{\sigma}'(\mathbf{x},\xi)=\mathcal{O}(|\mathbf{x}-\xi|^{-2})\quad \text{as } \mathbf{x}\to\xi \tag{18b}$$

$$\lim_{\eta\to 0}\int_{\mathscr{R}\cap\partial B_\eta(\xi)=\Lambda_\eta(\xi)}\mathbf{t}'(\mathbf{x},\xi)\mathrm{d}A_x=\mathbf{I} \tag{18c}$$

wherel $\mathbf{t}'$ are the tractions on the side of $\Lambda_\eta(\xi)$ that faces ξ

State $\mathscr{S}$(regular state):

$$\mathscr{S}=[\mathbf{u},\boldsymbol{\sigma}]\in\mathscr{E}_s(E,\nu,\mathbf{f};\bar{\mathscr{R}}-\{\xi\}),\quad \mathbf{f}\in\mathscr{C}(\bar{\mathscr{R}}) \tag{18d}$$

If $\mathbf{t}'(\mathbf{x},\xi)=\boldsymbol{\sigma}'(\mathbf{x},\xi)\cdot\mathbf{n}(\mathbf{x})$, $\mathbf{t}(\mathbf{x},\xi)=\boldsymbol{\sigma}(\mathbf{x},\xi)\cdot\mathbf{n}(\mathbf{x})$ and from (5), the following identity holds:

$$\begin{aligned}\mathbf{I}\cdot\mathbf{u}(\xi)+\int_{\partial\mathscr{R}}\mathbf{t}'(\mathbf{x},\xi)\cdot\mathbf{u}(\mathbf{x})\,\mathrm{d}A_x+\int_{\mathscr{R}-\{\xi\}}\mathbf{f}'(\mathbf{x})\cdot\mathbf{u}(\mathbf{x})\,\mathrm{d}V_x\\ =\int_{\partial\mathscr{R}}\mathbf{t}(\mathbf{x})\cdot\mathbf{u}'(\mathbf{x},\xi)\,\mathrm{d}A_x+\int_{\mathscr{R}-\{\xi\}}\mathbf{f}(\mathbf{x})\cdot\mathbf{u}'(\mathbf{x},\xi)\,\mathrm{d}V_x\end{aligned} \tag{19}$$

4.1. Somigliana's identity for the three-dimensional layer state

The specialization of equation (19) using the three-dimensional fundamental solution for a point load in an infinite layer of uniform thickness will now be presented.

Let $\mathbf{X}=\{0;\mathbf{e}_1,\mathbf{e}_2,\mathbf{e}_3\}$ and let $\mathscr{P}\subset E_3$ be the infinite layer region of uniform thickness h as defined in (6). Let $\partial\mathscr{P}_1$ and $\partial\mathscr{P}_2$ denote the two infinite planar surfaces of the region (see Figure 2).

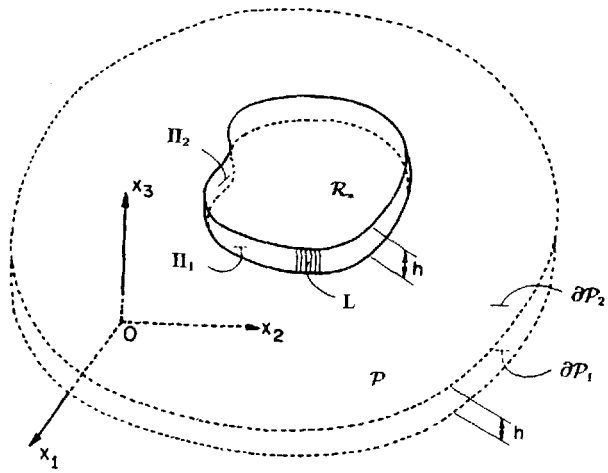

Figure 2. Schematic of the regular cylindrical region $\mathcal{R}_* \subset \mathcal{P}$

Let $\bar{\mathcal{R}}_*$ be the closure of the regular region $\mathcal{R}_* \subset \mathcal{P}$ with uniform thickness h, and let Π_1 and Π_2 be the *terminal* cross-sections of $\bar{\mathcal{R}}_*$. Further, let $\Pi_1 \subset \partial\mathcal{P}_1$ and $\Pi_2 \subset \partial\mathcal{P}_2$ (see Figure 2). Let $\partial\mathcal{R}_*$ be the surface of $\mathcal{R}_*$. Then the lateral boundary of $\mathcal{R}_*$ will be defined as follows:

$$L = \partial\mathcal{R}_* - (\Pi_1 \cup \Pi_2) \tag{20}$$

In the following discussion we choose to identify the arbitrary region $\mathcal{R}$ in equation (19) with the regular region $\mathcal{R}_*$.

We also choose to identify the singular state $\mathcal{S}'$ in (18) with the fundamental solution for the point load in the infinite layer. We thus get.

$$\mathcal{S}' = [\mathbf{u}', \boldsymbol{\sigma}'] = \mathcal{S}^k(\mathbf{x}, \boldsymbol{\xi}) = \mathcal{S}(\mathbf{x}, \boldsymbol{\xi}, \mathbf{l} = \mathbf{e}_k), \quad k = 1, 2, 3 \tag{21}$$

In addition, we restrict $\boldsymbol{\xi}$ to be in the *interior* or $\mathcal{R}_*$. The above are indeed appropriate choices, since $\mathcal{S}^k(\mathbf{x}, \boldsymbol{\xi})$ satisfies properties (7a)–(7d) for $\mathbf{l} = \mathbf{e}_k$ and thus also satisfies the restrictions (18a)–(18c), and also since, by construction, $\bar{\mathcal{R}}_* \subset \mathcal{P}$.

In addition, $\mathbf{f}' = \mathbf{0}$ on $\bar{\mathcal{R}}_* - \{\boldsymbol{\xi}\}$. Also since $\boldsymbol{\xi} \in \mathring{\mathcal{R}}_*$, then by (7b) we have

$$\mathbf{t}'(\mathbf{x}, \boldsymbol{\xi}) = \mathbf{t}^k(\mathbf{x}, \boldsymbol{\xi}) = \mathbf{0}, \quad \forall \mathbf{x} \in \Pi_\alpha \ (\alpha = 1, 2) \tag{22}$$

Finally, as in (19) the second state

$$\mathcal{S} = [\mathbf{u}(\mathbf{x}), \boldsymbol{\sigma}(\mathbf{x})] = \mathcal{E}_s(E, \nu, \mathbf{f}; \bar{\mathcal{R}}_*) \tag{23}$$

is taken to be a regular (non-singular) elastostatic state defined on the region $\bar{\mathcal{R}}_*$. From the above, equation (19) reduces to

$$u_k(\boldsymbol{\xi}) = -\int_L [\boldsymbol{\sigma}^k(\mathbf{x}, \boldsymbol{\xi}) \cdot \mathbf{n}(\mathbf{x})] \cdot \mathbf{u}(\mathbf{x}) \, dA_x + \int_{L \cup \Pi_1 \cup \Pi_2} [\boldsymbol{\sigma}(\mathbf{x}) \cdot \mathbf{n}(\mathbf{x})] \cdot \mathbf{u}^k(\mathbf{x}, \boldsymbol{\xi}) \, dA_x$$
$$+ \int_{\mathcal{R}_* - \{\boldsymbol{\xi}\}} \mathbf{f}(\mathbf{x}) \cdot \mathbf{u}^k(\mathbf{x}, \boldsymbol{\xi}) \, dV_x \tag{24}$$

where $u_k(\boldsymbol{\xi}) = \mathbf{u}(\boldsymbol{\xi}) \cdot \mathbf{e}_k$ for $\boldsymbol{\xi} \in \mathring{\mathcal{R}}_*$.

Expression (24) provides the components of the displacement field for the non-singular state $\mathcal{S}$ at points *interior* of the regular region $\mathcal{R}_*$. These are given with respect to the displacement and

tractions of $\mathscr{S}$ at the boundary $\partial\mathscr{R}_*$ and the three-dimensional fundamental solution for the point load in an infinite layer of uniform thickness obtained by Benitez and Rosakis.[9]

$\mathscr{R}_*$ is a regular subset of $\mathscr{P}$ (infinite layer of uniform thickness) and is shown in Figure 2. It is worth noting here that the first integral of (24) involves integration only over the *lateral* surface of the region $\mathscr{R}_* \subset \mathscr{P}$.

It is very important to point out here that the displacement field, in the interior of the region, can be obtained once the displacement and traction on the lateral surface of the region are determined. Because of the special fundamental solution and the traction-free boundary conditions in both the singular and the regular states, the integrals on the two planar surfaces of the region $\mathscr{R}$ of the regular state are not necessary, which is advantageous in the numerical implementation, which will be discussed later.

4.2. *Stress field integral identity for the three-dimensional layer state*

The translation identity of equation (16) implies that

$$\frac{\partial}{\partial \xi_m}\mathbf{u}^k(\mathbf{x},\boldsymbol{\xi}) = -\frac{\partial}{\partial x_m}\mathbf{u}^k(\mathbf{x},\boldsymbol{\xi}) = -\mathbf{u}^{km}(\mathbf{x},\boldsymbol{\xi}) \tag{25}$$

and

$$\frac{\partial}{\partial \xi_m}\boldsymbol{\sigma}^k(\mathbf{x},\boldsymbol{\xi}) = -\frac{\partial}{\partial x_m}\boldsymbol{\sigma}^k(\mathbf{x},\boldsymbol{\xi}) = -\boldsymbol{\sigma}^{km}(\mathbf{x},\boldsymbol{\xi})$$

Differentiation of relation (24) and use of property (25) gives

$$u_{k,m}(\boldsymbol{\xi}) = \int_L [\boldsymbol{\sigma}^{km}(\mathbf{x},\boldsymbol{\xi})\cdot\mathbf{n}(\mathbf{x})]\cdot\mathbf{u}(\mathbf{x})\,dA_x - \int_{L\cup\Pi_1\cup\Pi_2} [\boldsymbol{\sigma}(\mathbf{x})\cdot\mathbf{n}(\mathbf{x})]\cdot\mathbf{u}^{km}(\mathbf{x},\boldsymbol{\xi})\,dA_x$$
$$- \int_{\mathscr{R}_*-\{\boldsymbol{\xi}\}} \mathbf{f}(\mathbf{x})\cdot\mathbf{u}^{km}(\mathbf{x},\boldsymbol{\xi})\,dV_x \quad \forall\boldsymbol{\xi}\in\mathring{\mathscr{R}}_* \tag{26}$$

Define now a state as follows

$$\bar{\mathscr{S}}^{km}(\mathbf{x},\boldsymbol{\xi}) = [\bar{\mathbf{u}}^{km}(\mathbf{x},\boldsymbol{\xi}),\bar{\boldsymbol{\sigma}}^{km}\mathbf{x},\boldsymbol{\xi})]$$
$$= -\left[\frac{\nu E}{(1+\nu)(1-2\nu)}\mathscr{S}^{ll}(\mathbf{x},\boldsymbol{\xi})\delta_{km} + \frac{E}{2(1+\nu)}[\mathscr{S}^{km}(\mathbf{x},\boldsymbol{\xi}) + \mathscr{S}^{mk}(\mathbf{x},\boldsymbol{\xi})]\right] \tag{27}$$

where $\mathscr{S}^{km}(\mathbf{x},\boldsymbol{\xi}) = \mathscr{S}^{k}_{,m}(\mathbf{x},\boldsymbol{\xi}) = [\mathbf{u}^{km}(\mathbf{x},\boldsymbol{\xi}),\boldsymbol{\sigma}^{km}(\mathbf{x},\boldsymbol{\xi})]$ is the three-dimensional layer *doublet* state described in Section 3.2. (14)–(17). Then (26) and (27) imply that.

$$\sigma_{km}(\boldsymbol{\xi}) = -\int_L [\bar{\boldsymbol{\sigma}}^{km}(\mathbf{x},\boldsymbol{\xi})\cdot\mathbf{n}(\mathbf{x})]\cdot\mathbf{u}(\mathbf{x})\,dA_x + \int_{L\cup\Pi_1\cup\Pi_2} [\boldsymbol{\sigma}(\mathbf{x})\cdot\mathbf{n}(\mathbf{x})]\cdot\bar{\mathbf{u}}^{km}(\mathbf{x},\boldsymbol{\xi})\,dA_x$$
$$+ \int_{\mathscr{R}_*-\{\boldsymbol{\xi}\}} \mathbf{f}(\mathbf{x})\cdot\bar{\mathbf{u}}^{km}(\mathbf{x},\boldsymbol{\xi})\,dV_x, \quad \forall\boldsymbol{\xi}\in\mathring{\mathscr{R}}_* \tag{28}$$

Expression (28) provides the components of the stress field for the regular state $\mathscr{S}$ at points *interior* to the region $\mathscr{R}_*$. $\mathscr{R}_*$ is the regular subset of $\mathscr{P}$ (infinite layer of uniform thickness) as defined in Section 4.1 and shown in Figure 2. The stress components are given with respect to the displacement and tractions on the boundary $\partial\mathscr{R}_*$ and the doublet state corresponding to the three-dimensional fundamental solution for a point load in an infinite layer of uniform thickness.

4.3. Displacement field integral identity for the three-dimensional layer state

Identity (24) for the displacements is restricted to points $\xi \in \mathring{\mathscr{R}}_*$ (interior of $\mathscr{R}_*$), in which case the tractions $\mathbf{t}^k(\mathbf{x}, \xi) = \boldsymbol{\sigma}^k(\mathbf{x}, \xi) \cdot \mathbf{n}(\mathbf{x})$ of the first integral are integrable over the surface. An expression similar to (24), for $\xi \in \partial\mathscr{R}_*$, is obtained directly from the reciprocal theorem (5) by defining the following region.

Let $\mathscr{R}_*(\eta) \in \mathscr{P}$ be a regular subset of $\mathscr{P}$ defined as follows:

$$\mathscr{R}_*(\eta) = \mathscr{R}_* - B_\eta(\xi) \quad \forall \eta > 0 \tag{29}$$

Then $\partial\mathscr{R}_*(\eta) = \partial\mathscr{R}_* - (\partial\mathscr{R}_* \cap B_\eta(\xi)) + \partial B_\eta(\xi) \cap \mathscr{R}_*$ (see Figure 3).

Point ξ is then by construction exterior to this region. Since $\mathscr{R}_*(\eta) \subset \mathscr{P}$, one can identify, in (5), state $\mathscr{S}'$ by $\mathscr{S}^k(\mathbf{x}, \xi)$ (the point load solution for the infinite layer), where $\xi \in \partial\mathscr{R}_*$, $\mathbf{x} \in \mathscr{R}_*(\eta)$. Since $\xi \notin \mathscr{R}_*(\eta)$, $\mathscr{S}^k(\mathbf{x}, \xi)$ is non-singular in $\mathscr{R}_*(\eta)$, for all $\eta > 0$. One can also identify $\mathscr{S}''$ as any regular elastostatic state where

$$\mathscr{S} = [\mathbf{u}(\mathbf{x}), \boldsymbol{\sigma}(\mathbf{x})] \in \mathscr{E}_s(E, \nu, \mathbf{f}, \bar{\mathscr{R}}_*), \quad \mathbf{f} \in \mathscr{C}(\mathscr{R}_*) \tag{30}$$

By construction, both choices $\mathscr{S}'$ and $\mathscr{S}''$ are elastostatic states in $\mathscr{R}_*(\eta)$ and we can write

$$\begin{aligned} \mathscr{S}' &= \mathscr{S}^k(\mathbf{x}, \xi) = [\mathbf{u}^k(\mathbf{x}, \xi), \boldsymbol{\sigma}^k(\mathbf{x}, \xi)] \in \mathscr{E}_s(E, \nu, \mathbf{0}, \mathscr{R}_*(\eta)) \quad \forall \xi \in \partial\mathscr{R}_* \ \forall \eta > 0 \\ \mathscr{S}'' &= \mathscr{S}(\mathbf{x}) = [\mathbf{u}(\mathbf{x}), \boldsymbol{\sigma}(\mathbf{x})] \in \mathscr{E}_s(E, \nu, \mathbf{f}, \mathscr{R}_*(\eta)) \quad \mathbf{f} \in \mathscr{C}(\mathscr{R}_*) \end{aligned} \tag{31}$$

The reciprocal theorem then gives

$$\begin{aligned} \int_{\partial B_\eta(\xi) \cap \mathscr{R}_*} \mathbf{t}^k(\mathbf{x}, \xi) \cdot \mathbf{u}(\mathbf{x}) \mathrm{d}A_x = & - \int_{\partial\mathscr{R}_* - (\partial\mathscr{R}_* \cap B_\eta(\xi))} \mathbf{t}^k(\mathbf{x}, \xi) \cdot \mathbf{u}(\mathbf{x}) \mathrm{d}A_x \\ & + \int_{\partial B_\eta(\xi) \cap \mathscr{R}_*} \mathbf{t}(\mathbf{x}) \cdot \mathbf{u}^k(\mathbf{x}, \xi) \mathrm{d}A_x \\ & + \int_{\partial\mathscr{R}_* - (\partial\mathscr{R}_* \cap B_\eta(\xi))} \mathbf{t}(\mathbf{x}) \cdot \mathbf{u}^k(\mathbf{x}, \xi) \mathrm{d}A_x \\ & + \int_{\mathscr{R}_* - B_\eta(\xi)} \mathbf{f}(\mathbf{x}) \cdot \mathbf{u}^k(\mathbf{x}, \xi) \mathrm{d}V_x \quad \forall \eta > 0 \ \forall \xi \in \partial\mathscr{R}_* \end{aligned} \tag{32}$$

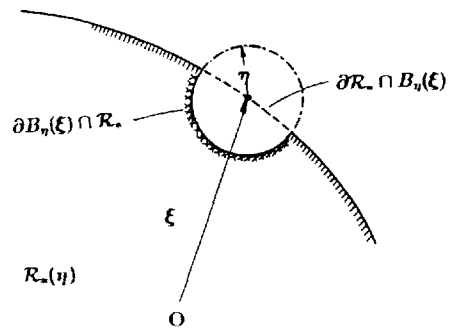

Figure 3. Schematic representation of the region $\mathscr{R}_*(\eta) = \mathscr{R}_* - B_\eta(\xi)$

We also recall property (7d) of $\mathscr{S}' = \mathscr{S}^k$ and the regularity (30) of $\mathscr{S}'' = \mathscr{S}$ on $\mathscr{R}_*$ which imply that there exist constants $K, L, M, N, Q, > 0$, such that

$$|\mathbf{u}| < K, \quad \|\boldsymbol{\sigma}\| < L, \quad |\mathbf{f}| < M \quad \text{on } \partial B_\eta(\xi) \cap \mathscr{R}_* \tag{33}$$

and

$$|\mathbf{u}^k| < \frac{N}{\eta}, \quad \|\boldsymbol{\sigma}^k\| < \frac{Q}{\eta^2} \quad \text{on } \partial B_\eta(\xi) \cap \mathscr{R}_* \text{ as } \eta \to 0$$

By means of the above properties, we can write

$$\int_{\partial B_\eta(\xi) \cap \mathscr{R}_*} [\boldsymbol{\sigma}(\mathbf{x}) \cdot \mathbf{n}(\mathbf{x})] \cdot \mathbf{u}^k(\mathbf{x}, \xi) \mathrm{d}A_x \leqslant 4\pi LN\eta \tag{34}$$

which implies that

$$\lim_{\eta \to 0} \int_{\partial B_\eta(\xi) \cap \mathscr{R}_*} \mathbf{t}(\mathbf{x}) \cdot \mathbf{u}^k(\mathbf{x}, \xi) \mathrm{d}A_x = 0 \tag{35}$$

Also because of the smoothness of $\mathbf{u}(\mathbf{x})$ (see (30)), we can write, for every $\mathbf{x} \in \partial B_\eta(\xi) \cap \mathscr{R}_*$,

$$\mathbf{u}(\mathbf{x}) = \mathbf{u}(\xi) + \nabla \mathbf{u}(\xi)(\mathbf{x} - \xi) + \mathscr{O}(|\mathbf{x} - \xi|^2) \quad \text{as } \eta \to 0 \tag{36}$$

This implies that there exists a constant $G > 0$, such that

$$|\mathbf{u}(\mathbf{x}) - \mathbf{u}(\xi)| \leqslant G\eta \quad \forall \mathbf{x} \in \partial B_\eta(\xi) \cap \mathscr{R}_*, \ \eta \to 0 \tag{37}$$

By using (36), one can write

$$\lim_{\eta \to 0} \int_{\partial B_\eta(\xi) \cap \mathscr{R}_*} \mathbf{t}^k(\mathbf{x}, \xi) \cdot \mathbf{u}(\mathbf{x}) \mathrm{d}A_x = \mathbf{u}(\xi) \cdot \left\{ \lim_{\eta \to 0} \int_{\partial B_\eta(\xi) \cap \mathscr{R}_*} \mathbf{t}^k(\mathbf{x}, \xi) \mathrm{d}A_x \right\} + \lim_{\eta \to 0} \int_{\partial B_\eta(\xi) \cap \mathscr{R}_*} \mathbf{t}^k(\mathbf{x}, \xi) \cdot [\mathbf{u}(\mathbf{x}) - \mathbf{u}(\xi)] \mathrm{d}A_x \tag{38}$$

Using (37) and (33), one can now show that the second term of (38) vanishes. This is demonstrated by observing that

$$\int_{\partial B_\eta(\xi) \cap \mathscr{R}_*} \mathbf{t}^k(\mathbf{x}, \xi) \cdot [\mathbf{u}(\mathbf{x}) - \mathbf{u}(\xi)] \mathrm{d}A_x \leqslant 4\pi QG\eta \quad \text{as } \eta \to 0 \tag{39}$$

This inequality and (38) imply that

$$\lim_{\eta \to 0} \int_{\partial B_\eta(\xi) \cap \mathscr{R}_*} \mathbf{t}^k(\mathbf{x}, \xi) \cdot \mathbf{u}(\mathbf{x}) \mathrm{d}A_x = \mathbf{u}(\xi) \cdot \left\{ \lim_{\eta \to 0} \int_{\partial B_\eta(\xi) \cap \mathscr{R}_*} \mathbf{t}^k(\mathbf{x}, \xi) \mathrm{d}A_x \right\} = \mathbf{u}(\xi) \cdot \mathbf{C}^k(\xi) \tag{40}$$

Taking the limit of (32) as $\eta \to 0$, using (35) and (40) and observing that $\lim_{\eta \to 0}[\partial \mathscr{R}_* \cap B_\eta(\xi)] = \partial \mathscr{R}_* - \{\xi\}$ and $\lim_{\eta \to 0}[\mathscr{R}_* \cap B_\eta(\xi)] = \mathscr{R}_* - \{\xi\}$, we get

$$\mathbf{u}(\xi) \cdot \mathbf{C}^k(\xi) = -\int_{\partial \mathscr{R}_* - \{\xi\}} \mathbf{t}^k(\mathbf{x}, \xi) \cdot \mathbf{u}(\mathbf{x}) \mathrm{d}A_x + \int_{\partial \mathscr{R}_* - \{\xi\}} \mathbf{t}(\mathbf{x}) \cdot \mathbf{u}^k(\mathbf{x}, \xi) \mathrm{d}A_x + \int_{\mathscr{R}_* - \{\xi\}} \mathbf{f}(\mathbf{x}) \cdot \mathbf{u}^k(\mathbf{x}, \xi) \mathrm{d}V_x \quad \forall \xi \in \partial \mathscr{R}_* \tag{41}$$

Observing finally that $\mathbf{t}^k(\mathbf{x},\boldsymbol{\xi}) = \mathbf{0}$ on $\Pi_\alpha - \{\boldsymbol{\xi}\}$ (see (7b)) and by replacing $\partial\mathscr{R}_*$ by L in the first integral of the above equation (41) reduces to

$$\mathbf{u}(\boldsymbol{\xi})\cdot\mathbf{C}^k(\boldsymbol{\xi}) = -\int_{L-\{\boldsymbol{\xi}\}} \mathbf{t}^k(\mathbf{x},\boldsymbol{\xi})\cdot\mathbf{u}(\mathbf{x})\,\mathrm{d}A_x + \int_{L\cup\Pi_1\cup\Pi_2-\{\boldsymbol{\xi}\}} \mathbf{t}(\mathbf{x})\cdot\mathbf{u}^k(\mathbf{x},\boldsymbol{\xi})\,\mathrm{d}A_x + \int_{\mathscr{R}_*-\{\boldsymbol{\xi}\}} \mathbf{f}(\mathbf{x})\cdot\mathbf{u}^k(\mathbf{x},\boldsymbol{\xi})\,\mathrm{d}V_x \quad \forall\boldsymbol{\xi}\in\partial\mathscr{R}_* \tag{42}$$

where

$$\mathbf{C}^k(\boldsymbol{\xi}) = \lim_{\eta\to 0}\int_{\partial B_\eta(\boldsymbol{\xi})\cap\mathscr{R}_*} \mathbf{t}^k(\mathbf{x},\boldsymbol{\xi})\,\mathrm{d}A_x \tag{43}$$

$\mathbf{C}^k(\boldsymbol{\xi})$ is a vector whose value depends on the nature of the stress of the fundamental solution $\mathscr{S}^k(\mathbf{x},\boldsymbol{\xi})$ and on the location of the position vector $\boldsymbol{\xi}$.

If $\boldsymbol{\xi}$ lies on one of the end cross-sections Π_α ($\boldsymbol{\xi}\in\Pi_\alpha\subset\partial\mathscr{P}_\alpha$) then $\partial B_\eta(\boldsymbol{\xi})\cap\mathscr{R}_* = \partial B_\eta(\boldsymbol{\xi})\cap\mathscr{P}$ and $\mathbf{C}^k(\boldsymbol{\xi}) = \mathbf{e}_k$. This follows immediately from the fact that (43) reduces to the first integral of (7c) for $\mathbf{l} = \mathbf{e}_k$. This is not true however for $\boldsymbol{\xi}\in L$, $\boldsymbol{\xi}\in\mathring{\mathscr{P}}$. In this case, the integral of (43) has to be evaluated directly by using the fundamental solution in question. In order to do so, it is important to recall at this point that the present fundamental solution (point load in an infinite layer of uniform thickness) was shown to reduce to the *Kelvin state* (point load of an infinite elastic body occupying E_3) at the limit of $\mathbf{x}\to\boldsymbol{\xi}$, $\boldsymbol{\xi}\in\mathring{\mathscr{P}}$ (see Reference 9). Given the above property, the integral of definition (43) reduces to the equivalent integral for the *Kelvin state* for $\boldsymbol{\xi}\in L$, $\boldsymbol{\xi}\in\mathring{\mathscr{P}}$. For the specific case of L being a *smooth* regular surface (a regular surface with a continuously turning tangent plane), it can be shown that $\mathbf{C}^k(\boldsymbol{\xi}) = \frac{1}{2}\mathbf{e}_k$ for $\boldsymbol{\xi}\in L$, $\boldsymbol{\xi}\in\mathring{\mathscr{P}}$. The proof of the above is entirely analogous to the equivalent result that appears in classical boundary element formulations using the *Kelvin solution*. Expressions for $\mathbf{C}^k(\boldsymbol{\xi})$ corresponding to choices of L containing sharp edges on corners are expressed as functions of the angles involved.[14]

4.4. *Integral identities for three-dimensional layer regions with traction free terminal cross-sections*

Here we discuss some important special cases of the integral identities (24), (28) and (42). These correspond to a class of three-dimensional boundary-value problems involving regions $\mathscr{R}_*$ whose terminal cross-sections Π_1, Π_2 are traction-free. We also discuss the special case of zero body forces ($\mathbf{f} = \mathbf{0}$ on $\mathscr{R}_*$). We choose the state $\mathscr{S}(\mathbf{x})$ corresponding to the problem under investigation to have the following properties:

$$\begin{aligned} &\mathscr{S}(\mathbf{x}) = [\mathbf{u}(\mathbf{x}),\boldsymbol{\sigma}(\mathbf{x})] = \mathscr{E}_s(E,\nu,\mathbf{0};\bar{\mathscr{R}}_*)\\ &\boldsymbol{\sigma}(\mathbf{x})\cdot\mathbf{n}(\mathbf{x}) = \hat{\mathbf{t}}(\mathbf{x}), \quad \forall\mathbf{x}\in L_t\\ &\boldsymbol{\sigma}(\mathbf{x})\cdot\mathbf{n}(\mathbf{x}) = \mathbf{0}, \quad \forall\mathbf{x}\in\Pi_\alpha\ (\alpha = 1,2) \end{aligned} \tag{44}$$

and

$$\mathbf{u}(\mathbf{x}) = \hat{\mathbf{u}}(\mathbf{x}), \quad \forall\mathbf{x}\in L_u$$

where $\partial\mathscr{R}_* = L\cup\Pi_1\cup\Pi_2$, $L = L_t\cup L_u$. We will also assume that the lateral boundary L of the region $\mathscr{R}_*$ is *smooth* (with unique tangent plane defined). The integral identity for the displacement at the surface of a regular region $\mathscr{R}_*$ whose end cross-sections are traction-free is obtained from (42) and (44) as

$$\mathbf{u}(\boldsymbol{\xi})\cdot\mathbf{C}^k(\boldsymbol{\xi}) = -\int_{L-\{\boldsymbol{\xi}\}} \mathbf{t}^k(\mathbf{x},\boldsymbol{\xi})\cdot\mathbf{u}(\mathbf{x})\,\mathrm{d}A_x + \int_{L-\{\boldsymbol{\xi}\}} \mathbf{t}(\mathbf{x})\cdot\mathbf{u}^k(\mathbf{x},\boldsymbol{\xi})\,\mathrm{d}A_x \tag{45}$$

where

$$\mathbf{C}^k(\xi) = \begin{cases} \mathbf{e}_k & \text{if } \xi \in \Pi_z \\ \frac{1}{2}\mathbf{e}_k & \text{if } \xi \in L,\ \xi \in \mathring{\mathscr{P}} \end{cases} \tag{46}$$

and $\mathbf{t}^k(\mathbf{x}, \xi) = \boldsymbol{\sigma}^k(\mathbf{x}, \xi) \cdot \mathbf{n}(\mathbf{x})$. The above identity relates the displacements of the *entire surface* of the region $\mathscr{R}_*$ to the tractions and displacements of *only* the lateral surface L. For the special case of $L = L_t$, $\mathbf{t}(\mathbf{x}) = \hat{\mathbf{t}}(\mathbf{x})$, $\mathbf{x} \in L_t$ (traction boundary conditions), (45) assumes a particularly simple form since the second integral is known *a priori*.

Similarly, use of (44) reduces the integral identities (24) and (28) for the displacement and stress fields for points in the interior of $\mathscr{R}_*$ to the following simple forms:

$$u_k(\xi) = -\int_L \mathbf{t}^k(\mathbf{x}, \xi) \cdot \mathbf{u}(\mathbf{x}) \mathrm{d}A_x + \int_L \mathbf{t}(\mathbf{x}) \cdot \mathbf{u}^k(\mathbf{x}, \xi) \mathrm{d}A_x \tag{47}$$

where $\xi \in \mathring{\mathscr{R}}_*$, $\mathbf{t}^k(\mathbf{x}, \xi) = \boldsymbol{\sigma}^k(\mathbf{x}, \xi) \cdot \mathbf{n}(\mathbf{x})$,

$$\sigma_{km}(\xi) = -\int_L \bar{\mathbf{t}}^{km}(\mathbf{x}, \xi) \cdot \mathbf{u}(\mathbf{x}) \mathrm{d}A_x + \int_L \mathbf{t}(\mathbf{x}) \cdot \bar{\mathbf{u}}^{km}(\mathbf{x}, \xi) \mathrm{d}A_x \tag{48}$$

where $\xi \in \mathring{\mathscr{R}}_*$, $\bar{\mathbf{t}}^{km}(\mathbf{x}, \xi) = \bar{\boldsymbol{\sigma}}^{km}(\mathbf{x}, \xi) \cdot \mathbf{n}(\mathbf{x})$. All of the above identities involve integrals evaluated *only over the lateral surface of the region* $\mathscr{R}_*$.

5. NUMERICAL IMPLEMENTATION OF BOUNDARY INTEGRAL EQUATIONS

In the solution of a particular solid mechanics problems, the solid boundary and the boundary data will be approximate in order to solve the boundary integral equations (42) or (45) numerically. The approximations involve replacing the lateral boundary (L) and the portion over which the traction might be defined on the lower and upper surfaces (Π_z) by a complete set of surfaces patches, the so-called boundary elements. The boundary data are then interpolated over each boundary element. In cases that body forces are presented, the volume integrals imply a discretization process of the interior of the considered region in a similar way to the finite element method. In this case, the advantages of the boundary element method are lost. Nevertheless, when body forces correspond to the existence of gravity, angular acceleration and other potential fields, the volume integrals can be transformed into surface integrals, in a way similar to that developed by Stippes and Rizzo,[15] which can be treated numerically in an analogous way to the other integral terms in the boundary equation (42). The discretized form of equations (42) or (45) for every nodal point yields a system of linear algebraic equations. Once the boundary conditions are imposed, the system can be solved to obtain all the unknown values. Consequently, an approximate solution to the boundary value problem is obtained

For the sake of simplicity, we will study the case of zero body forces and traction free terminal cross-sections. Also the boundary elements in this investigation are taken to be flat in the process of discretization, and the boundary data are taken from the element centroid. In other words, *constant elements* are used.

It is now more convenient to work with matrix notation rather than carry on with the indicial notation. To this effect, we can start by defining the displacement and the traction vectors that apply over the element j by the values at its centroid, i.e.

$$\left.\begin{aligned} \mathbf{u}(\mathbf{x}) &= \{\mathbf{u}\}^j \\ \mathbf{t}(\mathbf{x}) &= \{\mathbf{t}\}^j \end{aligned}\right\} \quad \forall \mathbf{x} \in \text{element } j \tag{49}$$

where the superscript j denotes the element, and $\{\mathbf{u}\}^j$ and $\{\mathbf{t}\}^j$ indicate the displacement and traction vectors at the element centroid, respectively. They are usually called the element nodal values.

Let us now construct two matrices involving traction and displacement components of the fundamental solution as follows:

$$[\mathbf{t}^k(\mathbf{x},\boldsymbol{\xi})] = [\mathbf{t}^*(\mathbf{x},\boldsymbol{\xi})] = \begin{pmatrix} t_1^1(\mathbf{x},\boldsymbol{\xi}) & t_2^1(\mathbf{x},\boldsymbol{\xi}) & t_3^1(\mathbf{x},\boldsymbol{\xi}) \\ t_1^2(\mathbf{x},\boldsymbol{\xi}) & t_2^2(\mathbf{x},\boldsymbol{\xi}) & t_3^2(\mathbf{x},\boldsymbol{\xi}) \\ t_1^3(\mathbf{x},\boldsymbol{\xi}) & t_2^3(\mathbf{x},\boldsymbol{\xi}) & t_3^3(\mathbf{x},\boldsymbol{\xi}) \end{pmatrix} \tag{50}$$

$$[\mathbf{u}^k(\mathbf{x},\boldsymbol{\xi})] = [\mathbf{u}^*(\mathbf{x},\boldsymbol{\xi})] = \begin{pmatrix} u_1^1(\mathbf{x},\boldsymbol{\xi}) & u_2^1(\mathbf{x},\boldsymbol{\xi}) & u_3^1(\mathbf{x},\boldsymbol{\xi}) \\ u_1^2(\mathbf{x},\boldsymbol{\xi}) & u_2^2(\mathbf{x},\boldsymbol{\xi}) & u_3^2(\mathbf{x},\boldsymbol{\xi}) \\ u_1^3(\mathbf{x},\boldsymbol{\xi}) & u_2^3(\mathbf{x},\boldsymbol{\xi}) & u_3^3(\mathbf{x},\boldsymbol{\xi}) \end{pmatrix} \tag{51}$$

Suppose that the unit concentrated load is acting at the centroid ($\boldsymbol{\xi}^i$) of the ith element. Substitute the above functions into equation (45), and discretize the boundary to obtain the equation corresponding to the displacement vector at the nodal point i,

$$[C]\{\mathbf{u}\}^i + \sum_{j=1}^{\mathrm{NE}} \int_{\mathscr{L}_j} [\mathbf{t}^*(\mathbf{x},\boldsymbol{\xi}^i)]\{\mathbf{u}\}^j \mathrm{d}A_x = \sum_{j=1}^{\mathrm{NE}} \int_{\mathscr{L}_j} [\mathbf{u}^*(\mathbf{x},\boldsymbol{\xi}^i)]\{\mathbf{t}\}^j \mathrm{d}A_x \tag{52}$$

where $\mathscr{L}_j$ is the surface of the jth element, NE stands for the number of elements used and $[C]$ is equal to

$$[C] = \begin{pmatrix} \frac{1}{2} & 0 & 0 \\ 0 & \frac{1}{2} & 0 \\ 0 & 0 & \frac{1}{2} \end{pmatrix} \tag{53}$$

Since $\{\mathbf{u}\}^j$ and $\{\mathbf{t}\}^j$ are constants over the jth element, they can be taken out of the integral. Thus,

$$[C]\{\mathbf{u}\}^i + \sum_{j=1}^{\mathrm{NE}} \left(\int_{\mathscr{L}_j} [\mathbf{t}^*(\mathbf{x},\boldsymbol{\xi}^i)] \mathrm{d}A_x \right) \{\mathbf{u}\}^j = \sum_{j=1}^{\mathrm{NE}} \left(\int_{\mathscr{L}_j} [\mathbf{u}^*(\mathbf{x},\boldsymbol{\xi}^i)] \mathrm{d}A_x \right) \{\mathbf{t}\}^j \tag{54}$$

Equation (54) corresponds to a particular node i (centroid of element i). Once the terms are integrated, it can be written as

$$[C]\{\mathbf{u}\}^i + \sum_{j=1}^{\mathrm{NE}} [\hat{\mathbf{H}}^{ij}]\{\mathbf{u}\}^j = \sum_{j=1}^{\mathrm{NE}} [\mathbf{G}^{ij}]\{\mathbf{t}\}^j \tag{55}$$

where the superscript i denotes the position of the unit concentrated load (on the centroid of element i), and j indicates the element centroid at which the response is computed. Both i and j vary from 1 to NE. The influence matrices $[\hat{\mathbf{H}}^{ij}]$ and $[\mathbf{G}^{ij}]$ are 3×3 matrices and are defined as

$$[\hat{\mathbf{H}}^{ij}] = \int_{\mathscr{L}_j} [\mathbf{t}^*(\mathbf{x},\boldsymbol{\xi}^i)] \mathrm{d}A_x \tag{56}$$

$$[\mathbf{G}^{ij}] = \int_{\mathscr{L}_j} [\mathbf{u}^*(\mathbf{x},\boldsymbol{\xi}^i)] \mathrm{d}A_x \tag{57}$$

By examining (55), the following holds:

$$[\mathbf{H}^{ij}] = [\hat{\mathbf{H}}^{ij}] \quad \text{if } i \neq j$$
$$[\mathbf{H}^{ij}] = [\hat{\mathbf{H}}^{ij}] + [\mathbf{C}] \quad \text{if } i = j \tag{58}$$

Equation (55) for node i then becomes

$$\sum_{j=1}^{NE} [\mathbf{H}^{ij}]\{\mathbf{u}\}^j = \sum_{j=1}^{NE} [\mathbf{G}^{ij}]\{\mathbf{t}\}^j \tag{59}$$

Similarly, the contribution for all the nodes can be written. The equations can then be assembled into the global system of equations according to the nodes, i.e.

$$[\mathbf{H}]\{\mathbf{u}\} = [\mathbf{G}]\{\mathbf{t}\} \tag{60}$$

Matrices $[\mathbf{H}]$ and $[\mathbf{G}]$ are both $3NE \times 3NE$ matrices, $\{\mathbf{u}\}$ and $\{\mathbf{t}\}$ are $3NE \times 1$ vectors.

In the actual situations, the full $[\mathbf{H}]$ and $[\mathbf{G}]$ matrices are never stored according to these sizes. As the system of equations is generated, the known boundary conditions are multiplied out to generate the right-hand side vector; the coefficients of the unknown terms, either the displacement components or the traction components, populate the coefficient matrix $[\mathbf{A}]$,

$$[\mathbf{A}]\{\mathbf{x}\} = \{\mathbf{b}\} \tag{61}$$

where $[\mathbf{A}]$ is a $3NE \times 3NE$ matrix, $\{\mathbf{x}\}$ is a vector of unknowns and $\{\mathbf{b}\}$ is the known right-hand side. $\{\mathbf{x}\}$ and $\{\mathbf{b}\}$ are both $3NE \times 1$ vectors. Equation (61) is the actual form of equations that is to be solved. The Gauss matrix reduction method will be used to solve the equations.

5.1. Element matrices construction

The evaluation of the element matrices $[\hat{\mathbf{H}}^{ij}]$ and $[\mathbf{G}^{ij}]$ is crucial to the boundary element formulation. Since the components of the matrices involve the integration of the fundamental solution, and since the expressions of the three-dimensional layer fundmental solution are very complex, the integrals cannot be computed analytically.

One way to evaluate the matrix components is to use the Gaussian quadrature scheme. However, when an element is very close to the unit concentrated load or when the load is on the element,the singular nature of the fundamental solution yields high numerical values, and the variation of the fundamental solution over the integrated element is very high. In such cases, the Gaussian quadrature is effective only if many Gaussian points are needed. Two different alternatives have been used to evaluate the matrix components. The first one is a purely numerical procedure, while the second is an hybrid numerical–analytical one.

5.1.1. Purely numerical procedures The numerical integration of all the above components over an arbitrary element can be abstracted to the following simple expression:

$$w = \int_{\mathscr{Q}} f(\mathbf{x}, \boldsymbol{\xi})\, \mathrm{d}A_x \tag{62}$$

By using a mapping of the form

$$x_k = \sum_{I=1}^{I} N_I(\zeta, \eta) x_k^I \quad \forall k = 1, 2, 3 \tag{63}$$

where x_k, $\forall k = 1, 2, 3$, and (ζ, η) represent the global and local co-ordinate systems for a point

inside the generic element L, respectively, x_k^l represents the global co-ordinates of the I corners of the element and $N_l(\zeta, \eta)$ are the usual shape functions. Expression (62) becomes

$$w = \int_{-1}^{1} \int_{-1}^{1} \hat{f}(\zeta, \eta) |J(\zeta, \eta)| \, d\zeta \, d\eta \tag{64}$$

where $|J(\zeta, \eta)|$ is the Jacobian of the mapping and where

$$\hat{f}(\zeta, \eta) = f(\mathbf{x}(\zeta, \eta), \boldsymbol{\xi}(\zeta, \eta)) \tag{65}$$

By using the Gauss quadrature scheme,

$$w = \sum_{i=1}^{N} \sum_{j=1}^{N} \hat{f}(\zeta_i, \eta_i) |J(\zeta_i, \eta_j)| w_i w_j \tag{66}$$

where N is the number of integration points used, (ζ_i, η_j) $(i, j = 1, \ldots, N)$ are the positions of those points and w_i, w_j $(i, j = 1, \ldots, N)$ are the weights.

Equation (66) is the result of the numerical integration of function $f(\mathbf{x}, \boldsymbol{\xi})$ over an arbitrary element $\mathscr{L}$. Therefore, the evaluation of all the components in $[\mathbf{H}^{ij}]$ and $[\mathbf{G}^{ij}]$ can follow suit.

In order to compute the integral (62) with the reasonable accuracy, a high number of integration points should be placed on the element according to the element's distance from the integration node (element centroid for constant elements). One way to do this is by numerically subdividing the element into subelements. This is necessary when the fundamental solution is expected to vary highly in the element. The following are the rules for subdividing the most commonly used three-noded and four-noded elements, shown in Figure 4:

(i) Find the mid-points on the edges of an element, i.e. a, b, c and d for an element with four nodes or a, b and c for an element with three nodes.
(ii) Connect the mid-points of the opposite edges, as shown in Figure 4.

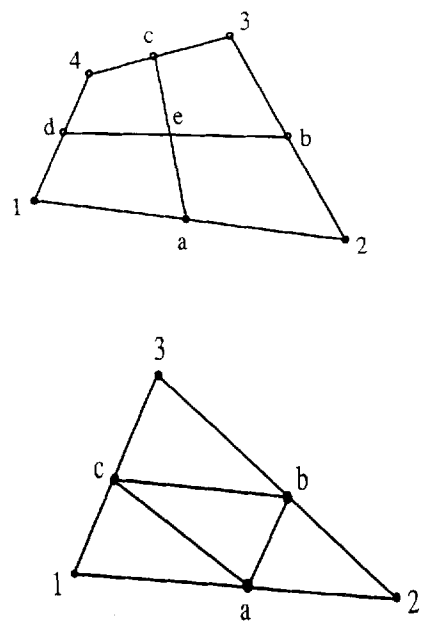

Figure 4. Subdivision of quadrilateral and triangular elements into four subelements

Several criteria have to be used in order to control the subdivision:

1. The length criterion. The subdivision stops when the distance between the loading point and the subelement is larger than or equal to C_{length} (a prechosen number) times the length of the smallest edge of the subdivided element.
2. The area criterion. The subdivision stops when the area of the smallest subelement is less than or equal to C_{area} (a prechosen number) times the area of the original element.
3. The above two criteria may both be in effect at the same time, such as in the case when the loading point is on an element or close to it.

It is important to point out that both criteria must be compatible; otherwise, the singularity properties of the fundamental solution cannot be captured. The compatibilities of the two criteria may also mean that they are not independent, i.e. if one criterion is chosen, the other criterion can be derived as a function of the first. This can be done by the following simple calculation.

Let d be the distance between the loading point and the element, L the typical length of the undivided element, l the typical length of the smallest subdivided element, C_{length} the chosen number for length criterion and C_{area} the chosen number for area criterion. Then the area of the undivided element is of the order of L^2 and the area of the smallest subdivided element is of the order of l^2.

From the length criterion $l = d/C_{\text{length}}$, while from the area criterion $l^2 = C_{\text{area}} \times L^2$.

In order for the two criteria to be imposed properly, the following equation has to be satisfied:

$$C_{\text{area}} = \left(\frac{d}{L \times C_{\text{length}}}\right)^2 \tag{67}$$

As an example, a four-noded element, as shown in Figure 5, is chosen. In this figure point p is the point at which the unit concentrated load is acting, while point q is the projection of p along the direction of the element normal onto the element.

Two subdivision cases will be depicted for different distances, d, between the loading point and the element. The length criterion will be set to $C_{\text{length}} = 2$ for all the cases.

Figure 6 shows the subdivisions for $d = 0{\cdot}0001$ and $d = 0{\cdot}1$, respectively.

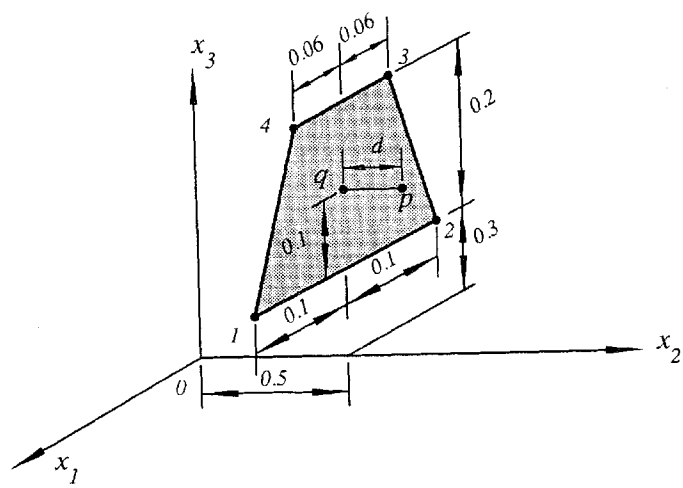

Figure 5. Dimensions of an element for numerical test

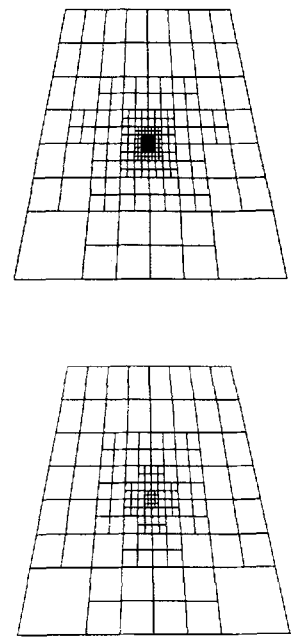

Figure 6. Quadrilateral elements subdivided into 640 (case $d = 10^{-4}$) and 148 (case 10^{-1}) subelements, respectively

5.1.2. Hybrid numerical–analytical procedure Due to the complexity of the fundamental solution, employment of many integration points, through a subdivision technique, would be very inefficient from a computational point of view. Therefore, an alternative way would be to evaluate the matrix components partially analytically and partially numerically. This idea can be mathematically expressed as follows:

$$[\hat{\mathbf{H}}^{ij}] = \int_{\mathscr{L}_j} [\mathbf{t}^* - \mathbf{t}_K]\, \mathrm{d}A_x + \int_{\mathscr{L}_j} [\mathbf{t}_K]\, \mathrm{d}A_x$$
$$[\mathbf{G}^{ij}] = \int_{\mathscr{L}_j} [\mathbf{u}^* - \mathbf{u}_K]\, \mathrm{d}A_x + \int_{\mathscr{L}_j} [\mathbf{u}_K]\, \mathrm{d}A_x \tag{68}$$

The subscript K denotes the Kelvin solution, while $\mathbf{t}^*$ and $\mathbf{u}^*$ are obtained from the three-dimensional layer fundamental solution. The first integral of each equation in (68) is to be integrated numerically, while the second integral of each equation is to be integrated analytically.

Although the fundamental solution and the Kelvin solution deal with totally different problems, they exhibit the same singular behaviour. When the unit concentrated load is acting in the interior of the infinite layer, the fundamental solution tends to the Kelvin solution as the point of observation approaches the loading point. Therefore, when the two points approach, the result of the subtraction of the fundamental solution by the Kelvin solution (first integral) tends to zero.

The analytical integration of the Kelvin solution over an arbitrary flat element was originally outlined by Cruse.[16]

Using the proposed hybrid evaluation of the components of the matrices $[\hat{\mathbf{H}}^{ij}]$ and $[\mathbf{G}^{ij}]$, one can take advantage of the above-mentioned analytical calculation and, thus, obtain the result with reasonable accuracy by using only a few Gauss quadrature points. This is because the

integrands of the first terms in equations (68) do not vary very much with distance. Consequently, a few integration points are expected to capture the variation well.

The above hypothesis can be verified by direct calculation by means of the purely numerical procedure.

Next, the integration of the three-dimensional layer fundamental solution over the same element shown in Figure 5 is computed using both the hybrid procedure and the purely numerical integration with subdivisions.

The materials properties are taken to be $E = 1$ and $\nu = 0{\cdot}3$. The thickness of the layer is chosen to be $h = 1$. Four, 16 and 36 points Gaussian quadrature schemes are used, and the results shown in Table I for the purely numerical procedure and in Table II for the hybrid procedure exhibit negligible differences.

The tremendous saving of computational effort introduced by the hybrid procedure is vital to the application of this boundary element method for computer-time-aware practitioners.

5.2. *Numerical evaluation of three-dimensional layer fundamental solution*

A close examination of the expressions for $u_i^k(\mathbf{x}, \boldsymbol{\xi})$ and $\sigma_{ij}^k(\mathbf{x}, \boldsymbol{\xi})$ presented in Appendix I reveals that all the expressions for the displacement and stress components can be cast in the general form shown below:

$$v(x_1, x_2, x_3) = A(E, \nu, h, x_1, x_2) \int_0^\infty \left\{ \frac{g'(\lambda, \chi, \psi)}{1 + e^{-4\lambda} - (2 + 4\lambda^2)^{-2\lambda}} J_\mu\left(\frac{\lambda\sqrt{x_1^2 + x_2^2}}{h}\right) - B(\nu, x_1, x_2, \chi, \psi) \frac{e^{-\lambda}}{\lambda^\alpha} \right\} d\lambda \tag{69}$$

where $v(x_1, x_2, x_3)$ may be a displacement or stress component, $\psi = H/h$ and $\chi = x_3/h$. The coefficients $A(E, \nu, h, x_1, x_2)$ and $B(\nu, x_1, x_2, \chi, \psi)$ are simple functions of the variables involved, the exponent α (1 or 2) depends on the component, $J_\mu(x)$ is the Bessel function of the order μ and $g'(\lambda, \chi, \psi)$ is a function composed of the finite summation of the products of the following form:

$$g'(\lambda, \chi, \psi) = \sum_{i=1}^{K} D_i \lambda^{\rho_i} \chi^{\beta_i} \psi^{\gamma_i} e^{\lambda(a_i\chi + b_i\psi + c_i)}, \tag{70}$$

where ρ_i, β_i, γ_i, a_i, b_i and c_i are integers. The parameter ρ_i may vary from 0 to 4, β_i and γ_i are either 0 or 1 and $a_i\chi + b_i\psi + c_i$ is always non-positive.

The second integrand in expression (69) eliminates the singularity in λ caused by the first one. If the first integrand is non-singular then $B = 0$. Hence, the solution is well behaved for every λ.

The basic idea of evaluating the stress and displacement components of the fundamental solution is to compute them partially analytically and partially numerically. To illustrate the idea, expression (69) is written in the following way:

$$v(x_1, x_2, x_3) = A(E, \nu, h, x_1, x_2) \left\{ \int_0^\infty g'(\lambda, \chi, \psi) J_\mu\left(\frac{\lambda\sqrt{x_1^2 + x_2^2}}{h}\right) d\lambda + \int_0^\infty \left[\left(\frac{g'(\lambda, \chi, \psi)}{1 + e^{-4\lambda} - (2 + 4\lambda^2)^{-2\lambda}} - g'(\lambda, \chi, \psi) \right) J_\mu\left(\frac{\lambda\sqrt{x_1^2 + x_2^2}}{h}\right) - B(\nu, x_1, x_2, \chi, \psi) \frac{e^{-\lambda}}{\lambda^\alpha} \right] d\lambda \right\} \tag{71}$$

Table I. Coefficients for $[G]$ and $[\hat{H}]$ matrices corresponding to purely numerical integration of 3-D layer fundamental solution for the element shown in Figure 5

Gaussian points Distance Elements	$[G^{ij}]$			$[\hat{H}^{ij}]$		
4	0·10946782154E + 00	0·00000000000E + 00	0·62072437847E − 15	0·50000000000E + 00	− 0·11173898612E − 10	0·00000000000E + 00
0	0·00000000000E + 00	0·87783800270E − 01	0·00000000000E + 00	0·11174977610E − 10	0·50000000000E + 10	0·27432589162E − 02
496	0·56338702421E − 15	0·00000000000E + 00	0·12687190679E + 00	0·00000000000E + 00	− 0·12588497925E − 01	0·50000000000E + 00
4	0·10934137090E + 00	− 0·73450462021E − 17	0·43944662227E − 15	0·49917474196E + 00	− 0·21275516071E − 13	− 0·20816681712E − 13
10^{-4}	− 0·73450462021E − 17	0·87748884184E − 01	0·15236001256E − 05	− 0·62803928724E − 13	0·49977751457E + 00	0·27449540317E − 02
484	0·41245591740E − 15	0·17360356150E − 05	0·12674424545E + 00	− 0·20920765120E − 13	− 0·12590099473E − 01	0·49925509116E + 00
4	0·97280653883E − 01	− 0·76436253160E − 17	0·26481638063E − 16	0·42712784185E + 00	− 0·10547118734E − 14	0·52041704279E − 15
10^{-2}	− 0·76436253160E − 17	0·84026350093E − 01	0·15057909577E − 03	− 0·81878948066E − 15	0·48509566017E + 00	0·30371187756E − 02
148	0·19786689648E − 17	0·17185463627E − 03	0·11462947392E + 00	− 0·24286128664E − 15	− 0·12193363593E − 01	0·43514840555E + 00
4	0·41621644483E − 01	0·17347234760E − 16	0·69388939039E − 17	0·78105461588E − 01	0·41633363423E − 16	0·97144514655E − 16
10^{-1}	0·17347234760E − 16	0·52618966618E − 01	0·51427223189E − 03	0·27755575616E − 16	0·26948369689E + 00	0·64574719768E − 02
16	0·86736173799E − 17	0·75755685385E − 03	0·56456525338E − 01	0·69388939039E − 16	− 0·31348210230E − 02	0·92864358138E − 01
16	0·10947198956E + 00	− 0·31566022603E − 26	0·46946462288E − 15	0·50000000913E + 00	0·53216112073E − 12	0·22778970794E − 21
0	− 0·31566022603E − 26	0·87786590579E − 01	− 0·15943614928E − 14	− 0·52343199219E − 12	0·50000000145E + 00	0·27430346741E − 02
496	0·37230655570E − 15	− 0·15895888690E − 14	0·12687486968E + 00	0·22861729245E − 21	− 0·12588281562E − 01	0·50000000789E + 00
16	0·10934306165E + 00	− 0·22615779692E − 17	0·45301100788E − 15	0·49926506677E + 00	− 0·21354445989E − 14	− 0·76119666126E − 14
10^{-4}	− 0·22615779692E − 17	0·87750037921E − 01	0·15231827340E − 05	− 0·78444195584E − 14	0·49985441813E + 00	0·27436584254E − 02
484	0·35076989599E − 15	0·17356187375E − 05	0·12674547481E + 00	− 0·95444485648E − 14	− 0·12588834827E − 01	0·49934639212E + 00
16	0·97280651007E − 01	− 0·15233040523E − 16	0·31604493328E − 16	0·42720753338E + 00	− 0·54123372450E − 15	0·49960036108E − 15
10^{-2}	− 0·15233040523E − 16	0·84025813790E − 01	0·15005192083E − 03	− 0·97144514655E − 15	0·48511517097E + 00	0·30189198697E − 02
148	0·39763114676E − 16	0·17132751332E − 03	0·11462725781E + 00	0·78409501114E − 15	− 0·12179129372E − 01	0·43512630651E + 00
16	0·41621953023E − 01	0·00000000000E + 00	− 0·26020852140E − 17	0·78108643220E − 01	0·13877787808E − 15	0·00000000000E + 00
10^{-1}	0·00000000000E + 00	0·52619150766E − 01	0·51426808461E − 03	− 0·22204460493E − 15	0·26945992104E + 00	0·64573375999E − 02
16	− 0·86736173799E − 18	0·75755444086E − 03	0·56457200223E − 01	− 0·55511151231E − 16	− 0·31349576557E − 02	0·92880278066E − 01
36	0·10947251149E + 00	0·54106490375E − 26	0·34045303469E − 15	0·50000002374E + 00	− 0·47581730223E − 12	− 0·17859863906E − 20
0	0·54106490375E − 26	0·87786911294E − 01	− 0·58782378312E − 16	0·47602893849E − 12	0·50000000764E + 00	0·27433289769E − 02
496	0·38410572466E − 15	− 0·51836124765E − 16	0·12687516735E + 00	− 0·16396852316E − 20	− 0·12588575865E − 01	0·50000003102E + 00
36	0·10934306060E + 00	− 0·11015663479E − 17	0·42517835227E − 15	0·49926501878E + 00	0·68512903684E − 14	− 0·13031242752E − 13
10^{-4}	− 0·11015663479E − 17	0·87750037875E − 01	0·15231818657E − 05	0·61894933623E − 14	0·49985439339E + 00	0·27436556411E − 02
484	0·35903693755E − 15	0·17356178693E − 05	0·12674547574E + 00	− 0·13933298959E − 13	− 0·12588832262E − 01	0·49934647679E + 00
36	0·97280650092E − 01	− 0·11763593571E − 16	0·51526708247E − 16	0·42720745874E + 00	− 0·24286128664E − 15	− 0·13877787808E − 15
10^{-2}	− 0·11763593571E − 16	0·84025813787E − 01	0·15005189111E − 03	− 0·80491169285E − 15	0·48511514734E + 00	0·30189038805E − 02
148	0·38055496254E − 16	0·17132748360E − 03	0·11462725880E + 00	0·38163916471E − 15	− 0·12179143533E − 01	0·43512639765E + 00
36	0·41621952966E − 01	0·17347234760E − 17	− 0·26020852140E − 17	0·78108641927E − 01	0·41633363423E − 16	− 0·13877787808E − 16
10^{-1}	0·17347234760E − 17	0·52619150341E − 01	0·51426808286E − 03	− 0·11102230246E − 15	0·26945988184E + 00	0·64573372475E − 02
16	0·69388939039E − 17	0·75755443911E − 03	0·56457200499E − 01	− 0·41633363423E − 16	− 0·31349579973E − 02	0·92880306711E − 01

Table 2. Coefficients for $[G]$ and $[\hat{H}]$ matrices corresponding to hybrid integration of 3-D layer fundamental solution for the element shown in Figure 5

Gaussian points Distance Elements	$[G^{ij}]$			$[\hat{H}^{ij}]$		
4	0·10947232874E + 00	0·00000000000E + 00	− 0·19081958236E − 16	0·50000000000E + 00	0·88817841970E − 15	0·00000000000E + 00
0	0·00000000000E + 00	0·87786613283E − 01	0·00000000000E + 00	0·44408920985E − 15	0·50000000000E + 00	0·27443316258E − 02
1	− 0·32959746044E − 16	0·00000000000E + 00	0·12687511722E + 00	0·00000000000E + 00	− 0·12576092402E − 01	0·50000000000E + 00
4	0·10934240983E + 00	− 0·10842021725E − 16	− 0·18214596498E − 15	0·49926501953E + 00	− 0·14432899320E − 14	0·00000000000E + 00
10^{-4}	− 0·10842021725E − 16	0·87749465571E − 01	0·15229688687E − 05	− 0·99920072216E − 15	0·49985439206E + 00	0·27443599427E − 02
1	− 0·17347234760E − 17	0·17350816216E − 05	0·12674519266E + 00	0·86736173799E − 18	− 0·12576050464E − 01	0·49934647619E + 00
4	0·97279999630E − 01	0·45102810375E − 16	0·18388068845E − 15	0·42720744703E + 00	0·17763568394E − 14	0·00000000000E + 00
10^{-2}	0·45102810375E − 16	0·84025241361E − 01	0·15003062067E − 03	0·17763568394E − 14	0·48511510585E + 00	0·30196057135E − 02
1	0·34694469520E − 17	0·17127385913E − 03	0·11462697725E + 00	− 0·55511151231E − 16	− 0·12166368302E − 01	0·43512633509E + 00
4	0·41621330947E − 01	0·55511151231E − 16	− 0·97578195524E − 17	0·78108559013E − 01	0·00000000000E + 00	0·11232334507E − 15
10^{-1}	0·62450045135E − 16	0·52618563032E − 01	0·51408977780E − 03	0·55511151231E − 15	0·26945943520E + 00	0·64578481125E − 02
1	− 0·12359904766E − 16	0·75702794672E − 03	0·56457054828E − 01	0·56812193838E − 16	− 0·31228299143E − 02	0·92879821480E − 01
16	0·10947283730E + 00	0·51275958839E − 29	0·31225022568E − 16	0·50000000000E + 00	− 0·34694469520E − 17	− 0·77623913074E − 27
0	0·51275958839E − 29	0·87787043395E − 01	− 0·23166730945E − 18	− 0·87777007884E − 15	0·50000000000E + 00	0·27437641305E − 02
1	0·45102810375E − 16	0·54604288484E − 17	0·12687535973E + 00	− 0·80779356695E − 27	− 0·12587545551E − 01	0·50000000000E + 00
16	0·10934291839E + 00	− 0·10965688535E − 16	− 0·17347234760E − 17	0·49926501965E + 00	0·11102230246E − 15	0·21684043450E − 17
10^{-4}	− 0·10965688535E − 16	0·87749895683E − 01	0·15231819571E − 05	− 0·24286128664E − 15	0·49985439212E + 00	0·27437924476E − 02
1	− 0·50306980803E − 16	0·17356178953E − 05	0·12674543517E + 00	0·30899761916E − 17	− 0·12587503612E − 01	0·49934647644E + 00
16	0·97280507877E − 01	0·78170976636E − 16	0·60715321659E − 16	0·42720745877E + 00	0·20122792321E − 15	0·71123662515E − 15
10^{-2}	0·76436253160E − 16	0·84025671596E − 01	0·15005189177E − 03	− 0·13877787808E − 16	0·48511511099E + 00	0·30190406958E − 02
1	0·29490299092E − 16	0·17132747774E − 03	0·11462721823E + 00	0·71123662515E − 15	− 0·12177814403E − 01	0·43512636018E + 00
16	0·41621810356E − 01	0·69822619908E − 16	− 0·80230960764E − 17	0·78108644960E − 01	0·65919492087E − 16	0·14007892069E − 15
10^{-1}	0·75894152074E − 16	0·52619007736E − 01	0·51426808861E − 03	0·63143934526E − 15	0·26945951600E + 00	0·64574745184E − 02
1	− 0·11492543028E − 16	0·75755438898E − 03	0·56457159801E − 01	0·56812193838E − 16	− 0·31335830511E − 02	0·92879932709E − 01
36	0·10947291300E + 00	0·88746851837E − 30	− 0·10842021725E − 16	0·50000000000E + 00	− 0·11622647289E − 15	− 0·29932094453E − 26
0	0·88746851837E − 30	0·87787119079E − 01	− 0·20972349865E − 17	0·42240516640E − 15	0·50000000000E + 00	0·27436913690E − 02
1	0·80230960764E − 17	0·50777147777E − 17	0·12687538130E + 00	− 0·29914838121E − 26	− 0·12588251960E − 01	0·50000000000E + 00
36	0·10934299409E + 00	− 0·10992793589E − 16	0·73725747729E − 17	0·49926501964E + 00	− 0·11874182193E − 14	0·11146953586E − 16
10^{-4}	− 0·10992370073E − 16	0·87749971367E − 01	0·15231819489E − 05	− 0·17659484985E − 14	0·49985439232E + 00	0·27437196861E − 02
1	− 0·36429192996E − 16	0·17356179525E − 05	0·12674545674E + 00	0·17028750372E − 16	− 0·12588210021E − 01	0·49934647664E + 00
36	0·97280583579E − 01	0·49141463468E − 16	0·46837533851E − 16	0·42720745843E + 00	0·74246164772E − 15	0·10386656812E − 14
10^{-2}	0·55212995634E − 16	0·84025747280E − 01	0·15005189095E − 03	0·82919782152E − 15	0·48511513062E + 00	0·30189679314E − 02
1	0·60498481225E − 16	0·17132748344E − 03	0·11462723980E + 00	0·87516799363E − 15	− 0·12178521059E − 01	0·43512638011E + 00
36	0·41621886269E − 01	0·60173220573E − 16	− 0·29598719309E − 16	0·78108643337E − 01	− 0·17433970934E − 15	0·70689981646E − 16
10^{-1}	0·53234326669E − 16	0·52619083645E − 01	0·51426808144E − 03	0·30531133177E − 15	0·26945971056E + 00	0·64574014707E − 02
1	− 0·30357660830E − 17	0·75755443768E − 03	0·56457181447E − 01	0·18648277367E − 16	− 0·31343138984E − 02	0·92880131494E − 01

Considering the first integral in the preceding expression, one has

$$\int_0^\infty g'(\lambda,\chi,\psi)J_\mu\left(\frac{\lambda\sqrt{x_1^2+x_2^2}}{h}\right)\mathrm{d}\lambda=\sum_{i=1}^{K}D_i\chi^{\beta_i}\psi^{\gamma_i}\int_0^\infty\lambda^{\rho_i}\mathrm{e}^{\lambda(a_i\chi+b_i\psi+c_i)}J_\mu\left(\frac{\lambda\sqrt{x_1^2+x_2^2}}{h}\right)\mathrm{d}\lambda \quad (72)$$

Each individual integral in the former expression can be computed analytically, and they can be expressed in the following form:

$$\int_0^\infty\lambda^a\mathrm{e}^{\ c\lambda}J_\mu(b\lambda)\mathrm{d}\lambda=G(\mu,a,b,c) \quad (73)$$

where a, b and c are not functions of λ and are non-negative. Expressions for $G(\mu,a,c,b)$ are found in Appendix II. Therefore, equation (71) can then be written in a more efficient way as follows:

$$\begin{aligned}v(x_1,x_2,x_3)=A(E,\nu,h,x_1,x_2)\Bigg\{&\sum_{i=1}^{K}D_i\chi^{\beta_i}\psi^{\gamma_i}G\left(\mu,\rho_i,\frac{\sqrt{x_1^2+x_2^2}}{h},-(a_i\chi+b_i\psi+c_i)\right)\\&+\int_0^\infty\left[\frac{(2+4\lambda^2-\mathrm{e}^{-2\lambda})\mathrm{e}^{-2\lambda}}{1+\mathrm{e}^{-4\lambda}-(2+4\lambda^2)\mathrm{e}^{-2\lambda}}g'(\lambda,\chi,\psi)J_\mu\left(\frac{\lambda\sqrt{x_1^2+x_2^2}}{h}\right)\right.\\&\left.-B(\nu,x_1,x_2,\chi,\psi)\frac{\mathrm{e}^{-\lambda}}{\lambda^\alpha}\right]\mathrm{d}\lambda\Bigg\}\end{aligned} \quad (74)$$

Define now

$$g(\lambda,\chi,\psi)=\mathrm{e}^{-2\lambda}g'(\lambda,\chi,\psi) \quad (75)$$

Then

$$g(\lambda,\chi,\psi)=\sum_{i=1}^{K}D_i\lambda^{\rho_i}\chi^{\beta_i}\psi^{\gamma_i}\mathrm{e}^{\lambda(a_i\chi+b_i\psi+c_i-2)}, \quad (76)$$

The most important feature in the previous expression is that $a_i\chi+b_i\psi+c_i-2$ is always negative, and it reaches its maximum at -2. This is a key feature which guarantees the convergence of the infinite integral in (74).

The integral in (74) cannot be evaluated analytically. It has to be evaluated numerically. After checking its denominator, one finds that it is not necessary to evaluate the integral over the entire integration region. Instead, it can be computed *approximately* over a region from 0 to P with relatively good accuracy for the first integrand. P is a preset *big* number. The integration interval is extended from 0 to $2P$ in order to achieve the same order of accuracy for the second part of the integrand. The error caused by truncating the integral will be discussed in the next section. The truncated version of (74) becomes

$$\begin{aligned}v(x_1,x_2,x_3)=A(E,\nu,h,x_1,x_2)\Bigg\{&\sum_{i=1}^{K}D_i\chi^{\beta_i}\psi^{\gamma_i}G\left(\mu,\rho_i,\frac{\sqrt{x_1^2+x_2^2}}{h},\right.\\&\left.-(a_i\chi+b_i\psi+c_i)\right)+\int_0^P\left[\frac{(2+4\lambda^2-\mathrm{e}^{-2\lambda})g(\lambda,\chi,\psi)}{1+\mathrm{e}^{-4\lambda}-(2+4\lambda^2)\mathrm{e}^{-2\lambda}}J_\mu\left(\frac{\lambda\sqrt{x_1^2+x_2^2}}{h}\right)\right.\\&\left.-B(\nu,x_1,x_2,\chi,\psi)\frac{\mathrm{e}^{-\lambda}}{\lambda^\alpha}\right]\mathrm{d}\lambda-B(\nu,x_1,x_2,\chi,\psi)\int_P^{2P}\frac{\mathrm{e}^{-\lambda}}{\lambda^\alpha}\mathrm{d}\lambda\Bigg\}\end{aligned} \quad (77)$$

By substituting (76) into (74) and performing variable transformation, one obtains

$$v(x_1,x_2,x_3) = A(E,v,h,x_1,x_2)\left\{\sum_{i=1}^{K} D_i\chi^{\beta_i}\psi^{\gamma_i}G\left(\mu,\rho_i,\frac{\sqrt{x_1^2+x_2^2}}{h},\right.\right.$$
$$\left. - (a_i\chi + b_i\psi + c_i)\right) + \int_0^P\left[\frac{2+4\lambda^2-e^{-2\lambda}}{1+e^{-4\lambda}-(2+4\lambda^2)e^{-2\lambda}}\sum_{i=1}^{K} D_i\lambda^{\rho_i}\right.$$
$$\chi^{\beta_i}\psi^{\gamma_i}e^{\lambda(a_i\chi+b_i\psi+c_i-2)}J_\mu\left(\frac{\lambda\sqrt{x_1^2+x_2^2}}{h}\right)$$
$$\left.\left. - B(v,x_1,x_2,\chi,\psi)\left(\frac{e^{-\lambda}}{\lambda^\alpha}+\frac{e^{-(\lambda+P)}}{(\lambda+P)^\alpha}\right)\right]d\lambda\right\} \tag{78}$$

The Gaussian quadrature scheme (GQS) is implemented to evaluate the integral. Since the integrand varies smoothly inside the integration interval, the interval is divided into equally sized integration subintervals. The size of the subinterval is crucial for the evaluation of an integral involving oscillatory Bessel functions. In order to determine the right size for the integration subintervals, the following parameter transformation is performed on the integration variable λ. Let

$$\lambda_1 = \lambda b \quad \text{and} \quad b = \frac{\sqrt{x_1^2+x_2^2}}{h} \tag{79}$$

For the sake of simplicity, we write λ in the place of λ_1; then (78) becomes

$$v(x_1,x_2,x_3) = A(E,v,h,x_1,x_2)\left\{\sum_{i=1}^{K} D_i\chi^{\beta_i}\psi^{\gamma_i}G(\mu,\rho_i,b,-(a_i\chi+b_i\psi+c_i))\right.$$
$$+\frac{1}{b}\int_0^{Pb}\left[\frac{2+4(\frac{\lambda}{b})^2-e^{-2(\lambda/b)}}{1+e^{-4(\lambda/b)}-(2+4(\frac{\lambda}{b})^2)e^{-2\lambda/b}}\sum_{i=1}^{K} D_i\left(\frac{\lambda}{b}\right)^{\rho_i}\right.$$
$$\left.\left.\times\chi^{\beta_i}\psi^{\gamma_i}e^{(\lambda/b)(a_i\chi+b_i\psi+c_i-2)}J_\mu(\lambda) - B(v,x_1,x_2,\chi,\psi)\left(\frac{e^{-(\lambda/b)}}{(\frac{\lambda}{b})^\alpha}+\frac{e^{-(\lambda/b+P)}}{(\frac{\lambda}{b}+P)^\alpha}\right)\right]d\lambda\right\} \tag{80}$$

The only oscillatory function in the integrand is the Bessel function $J_\mu(x)$. By examining the Bessel functions closely, one finds that although they are not periodic functions, they do have an approximate period of 2π as $x \to \infty$. Considering x to be greater than zero, the distance between the two adjacent zeros of the Bessel functions is greater than π. Therefore, it was decided to choose the size of the integration subinterval to be 3. Let N be the number of subintervals used. Then

$$N = \text{Int}[Pb/3] \tag{81}$$

where Int[a] stands for the closest integer to a, i.e. Int[a] = 1 for $a = 1{\cdot}2$ and Int[a] = 2 for $a = 1{\cdot}6$. The size of the integration subintervals is then Pb/N, and the subintervals are $[a_j, a_{j+1}]$ with $j = 1, \ldots, N$, where

$$a_i = \frac{Pb}{N}(i-1) \quad (i = 1, \ldots, N+1) \tag{82}$$

Define now

$$f(\mu, x_1, x_2, \alpha, \chi, \psi, \lambda) = \frac{2 + 4(\frac{\lambda}{b})^2 - e^{-2(\lambda/b)}}{1 + e^{-4(\lambda/b)} - (2 + 4(\frac{\lambda}{b})^2)e^{-2\lambda/b}} \sum_{i=1}^{K} D_i \left(\frac{\lambda}{b}\right)^{\rho_i}$$
$$\chi^{\beta_i}\psi^{\gamma_i} e^{(\lambda/b)(a_i\chi + b_i\psi + c_i - 2)} J_\mu(\lambda) - B(v, x_1, x_2, \chi, \psi)\left(\frac{e^{-(\lambda/b)}}{(\frac{\lambda}{b})^\alpha} + \frac{e^{-(\lambda/b + P)}}{(\frac{\lambda}{b} + P)^\alpha}\right) \tag{83}$$

Then

$$v(x_1, x_2, x_3) = A(E, v, h, x_1, x_2)\left\{\sum_{i=1}^{K} D_i \chi^{\beta_i}\psi^{\gamma_i} G(\mu, \rho_i, b, -(a_i\chi + b_i\psi + c_i))\right.$$
$$\left. + \frac{1}{b}\sum_{j=1}^{N}\int_{a_j}^{a_{j+1}} f(\mu, x_1, x_2, \alpha, \chi, \psi, \lambda)\,d\lambda\right\} \tag{84}$$

By performing the following variable transformation

$$\left.\begin{aligned} \lambda &= \frac{a_{j+1} + a_j}{2} + \frac{a_{j+1} - a_j}{2} t \\ d\lambda &= \frac{a_{j+1} - a_j}{2} dt \end{aligned}\right\} \quad (j = 1, \ldots, N) \tag{85}$$

expression (84) becomes

$$v(x_1, x_2, x_3) = A(E, v, h, x_1, x_2)\left\{\sum_{i=1}^{K} D_i \chi^{\beta_i}\psi^{\gamma_i} G(\mu, \rho_i, b, -(a_i\chi + b_i\psi + c_i))\right.$$
$$\left. + \sum_{j=1}^{N} \frac{a_{j+1} - a_j}{2b}\int_{-1}^{1} f\left(\mu, x_1, x_2, \alpha, \chi, \psi, \frac{a_{j+1} + a_j}{2} + \frac{a_{j+1} - a_j}{2} t\right) dt\right\} \tag{86}$$

The standard Gauss quadrature scheme can now be applied, yielding

$$v(x_1, x_2, x_3) = A(E, v, h, x_1, x_2)\left\{\sum_{i=1}^{K} D_i \chi^{\beta_i}\psi^{\gamma_i} G(\mu, \rho_i, b, -(a_i\chi + b_i\psi + c_i))\right.$$
$$\left. + \sum_{j=1}^{N} \frac{a_{j+1} - a_j}{2b} \sum_{k=1}^{M} f\left(\mu, x_1, x_2, \alpha, \chi, \psi, \frac{a_{j+1} + a_j}{2} + \frac{a_{j+1} - a_j}{2} t_k\right) w_k\right\} \tag{87}$$

where M is the number of integration points used and t_k and w_k, with $k = 1, \ldots, M$, are the positions and weights of these points, respectively.

The evaluation of (87) involving different number of integration points has been tested. It is found that a 36 Gaussian point scheme gives accurate results.

It should be emphasized once more that the numerical part of this integration is covergent due to the nature of the integrand (see (74)) while the remaining part can be evaluated in closed form. In addition, the accuracy of the integral in (80) will also depend on the choice of P.

5.2.1. Error analysis of the numerical evaluation. The error introduced in the evaluation of the stress and displacement components of the fundamental solution is mainly due to the numerical integration.

In order to perform an error analysis, expression (74) is rewritten in the following way:

$$v(x_1,x_2,x_3) = A(E,\nu,h,x_1,x_2)\Bigg\{\sum_{i=1}^{K} D_i\chi^{\beta_i}\psi^{\gamma_i}G(\mu,\rho_i,b,-(a_i\chi+b_i\psi+c_i))$$
$$+\int_0^P\Bigg[\frac{(2+4\lambda^2-e^{-2\lambda})e^{-2\lambda}}{1+e^{-4\lambda}-(2+4\lambda^2)e^{-2\lambda}}g'(\lambda,\chi,\psi)J_\mu\left(\frac{\lambda\sqrt{x_1^2+x_2^2}}{h}\right)$$
$$-B(\nu,x_1,x_2,\chi,\psi)\left(\frac{e^{-\lambda}}{\lambda^\alpha}+\frac{e^{-(\lambda+P)}}{(\lambda+P)^2}\right)\Bigg]d\lambda$$
$$+\int_P^\infty\frac{(2+4\lambda^2-e^{-2\lambda})e^{-2\lambda}}{1+e^{-4\lambda}-(2+4\lambda^2)e^{-2\lambda}}g'(\lambda,\chi,\psi)J_\mu\left(\frac{\lambda\sqrt{x_1^2+x_2^2}}{h}\right)d\lambda$$
$$-B(\nu,x_1,x_2,\chi,\psi)\int_{2P}^\infty\frac{e^{-\lambda}}{\lambda^\alpha}d\lambda\Bigg\} \tag{88}$$

Comparing the above formula with the proposed expression (78), it is found that the error in the numerical integration is mainly due to the truncation of the integration interval. The other part of the error appears because of the use of the Gaussian quadrature scheme. Define the error, ε, caused by the truncation of the integration interval as

$$\varepsilon=\Bigg|\int_P^\infty\Bigg[\frac{(2+4\lambda^2-e^{-2\lambda})e^{-2\lambda}}{1+e^{-4\lambda}-(2+4\lambda^2)e^{-2\lambda}}g'(\lambda,\chi,\psi)J_\mu\left(\frac{\lambda\sqrt{x_1^2+x_2^2}}{h}\right)d\lambda$$
$$-B(\nu,x_1,x_2,\chi,\psi)\int_{2P}^\infty\frac{e^{-\lambda}}{\lambda^\alpha}d\lambda\Bigg| \tag{89}$$

As indicated in (80), $g'(\lambda,\chi,\psi)$ is a summation of terms of the form $\lambda^{\rho_i}e^{\lambda(a_i\chi+b_i\psi+c_i)}$, with $i=1,\ldots,K$. Examining these terms carefully, one finds that the dominant term is the one with zero exponent. The coefficient of this term will be denoted as $D\lambda^\rho\chi^\beta\psi^\gamma$, in which ρ has a maximum value of 3.

Then the maximum error will be bounded by

$$\varepsilon\leqslant KD\chi^\beta\psi^\gamma\left|\int_P^\infty\frac{(2+4\lambda^2-e^{-2\lambda})e^{-2\lambda}}{1+e^{-4\lambda}-(2+4\lambda^2)e^{-2\lambda}}\lambda^3J_\mu(\lambda b)d\lambda\right|$$
$$+|B(\nu,x_1,x_2,\chi,\psi)|\left|\int_{2P}^\infty e^{-\lambda}d\lambda\right|$$
$$\leqslant KD\chi^\beta\psi^\gamma\int_P^\infty\left|\frac{(2+4\lambda^2-e^{-2\lambda})e^{-2\lambda}}{1+e^{-4\lambda}-(2+4\lambda^2)e^{-2\lambda}}\lambda^3\right||J_\mu(\lambda b)|d\lambda$$
$$+|B(\nu,x_1,x_2,\chi,\psi)|e^{-2P} \tag{90}$$

For any Bessel function $J_\mu(x)$, with μ integer, the following holds:

$$|J_\mu(x)|\leqslant 1,\quad 0\leqslant x\leqslant\infty \tag{91}$$

Consequently,

$$\varepsilon \leqslant KD\chi^{\beta}\psi^{\gamma}\int_{P}^{\infty}\left|\frac{(2+4\lambda^2-e^{-2\lambda})e^{-2\lambda}}{1+e^{-4\lambda}-(2+4\lambda^2)e^{-2\lambda}}\lambda^3\right|d\lambda + |B(v,x_1,x_2,\chi,\psi)|e^{-2P}$$

$$= KD\chi^{\beta}\psi^{\gamma}\int_{P}^{\infty}\frac{(2+4\lambda^2-e^{-2\lambda})e^{-2\lambda}}{1+e^{-4\lambda}-(2+4\lambda^2)e^{-2\lambda}}\lambda^3 d\lambda + |B(v,x_1,x_2,\chi,\psi)|e^{-2P} \quad (92)$$

Since $0 \leqslant 1+e^{-4\lambda}-(2+4\lambda^2)e^{-2\lambda} \leqslant 1+e^{-4P}-(2+4P^2)e^{-2P}$ for any $P>1$, the following holds:

$$\varepsilon \leqslant KD\chi^{\beta}\psi^{\gamma}\frac{1}{1+e^{-4P}-(2+4P^2)e^{-2P}}\int_{P}^{\infty}(2+4\lambda^2-e^{-2\lambda})e^{-2\lambda}\lambda^3 d\lambda + |B(v,x_1,x_2,\chi,\psi)|e^{-2P} \quad (93)$$

For $P=10$ and $P=20$, the error ε is of the order of 10^{-3} and 10^{-10}, respectively.

6. DISCUSSION AND CONCLUSIONS

In this work a specialization of the boundary element technique, which makes use of the three-dimensional fundamental solution for a point load acting in the interior of an infinite layer developed by Benitez and Rosakis,[8,9] is presented. This new formulation is specially suited for the treatment of three-dimensional problems whose geometries contain two parallel planar surfaces, such as in plate problems.

In general, the resulting integral identities (24), (28) and (42) contain surface integrals evaluated only over the *lateral* surface L of the *plate* region of interest. In addition, they also contain surface integrals evaluated exclusively over the portions of the two parallel planer surfaces (Π_1, Π_2) in which tractions are prescribed. In case where the two parallel planes are traction-free, the integral identities (45), (47) and (48) only contain integrals evaluated over the lateral surfaces of the region. From a numerical point of view, this makes the case of the identities very attractive for implementation in numerical boundary element formulations.

For problems with a traction-free boundary condition on the two planar surfaces, numerical solution of boundary-value problems involving such a scheme need only feature the discretization of the lateral surfaces of the region, no elements are needed for the parallel planar surfaces.

This formulation is very attractive in the solution of three-dimensional problems involving cavities such as holes, surface cracks, through cracks, flaws and defects in plates of uniform thickness. In such cases, the proposed formulation would require discretization over the cavity surfaces and the remaining parts of the lateral boundary. This results in a considerable saving in the number of elements required to capture the details of the three-dimensional deformation fields at the vicinity of stress concentrations. It also provides an attractive alternative to the classical boundary element (based on Kelvin's solution) and finite element methods.

ACKNOWLEDGEMENTS

The authors thank Prof. T. A. Cruse for many useful discussions on the analytical integration of the Kelvin solution. A. J. Rosakis acknowledges the support of the National Science Foundation

through the Presidential Young Investigator award *MSM*8451204. F. G. Benitez is grateful for the support of the Spanish Ministry of Education and Science through grants CICYT PA86-0310 and CICYT MAT91-1014.

APPENDIX I

The stress and displacement components corresponding to the state $\mathscr{S}^k(\mathbf{x},\xi) = [\mathbf{u}^k(\mathbf{x},\xi);\boldsymbol{\sigma}^k(\mathbf{x},\xi)]$ are presented as

$$\sigma^1_{11}(x_1,x_2,x_3) = \frac{v}{1-v}\sigma^1_{33}(x_1,x_2,x_3) + \frac{1}{16\pi(1-v)^2h^2}\frac{x_1}{\sqrt{x_1^2+x_2^2}}\left\{(1-v)\frac{x_1^2-3x_2^2}{x_1^2+x_2^2}\right.$$
$$\times\int_{\lambda=0}^{\lambda=\infty}\lambda[f_1(\lambda)-f_2(\lambda)]J_3\left(\frac{\lambda\sqrt{x_1^2+x_2^2}}{h}\right)\mathrm{d}\lambda$$
$$\left.-\int_{\lambda=0}^{\lambda=\infty}\lambda[(3+v)f_1(\lambda)+(1-v)f_2(\lambda)+4f_3(\lambda)]J_1\left(\frac{\lambda\sqrt{x_1^2+x_2^2}}{h}\right)\mathrm{d}\lambda\right\} \tag{94}$$

$$\sigma^1_{12}(x_1,x_2,x_3) = -\frac{1}{16\pi(1-v)h^2}\frac{x_2}{\sqrt{x_1^2+x_2^2}}\left\{\frac{x_2^2-3x_1^2}{x_1^2+x_2^2}\right.$$
$$\times\int_{\lambda=0}^{\lambda=\infty}\lambda[f_1(\lambda)-f_2(\lambda)]J_3\left(\frac{\lambda\sqrt{x_1^2+x_2^2}}{h}\right)\mathrm{d}\lambda$$
$$\left.+\int_{\lambda=0}^{\lambda=\infty}\lambda[f_1(\lambda)+f_2(\lambda)+2f_3(\lambda)]J_1\left(\frac{\lambda\sqrt{x_1^2+x_2^2}}{h}\right)\mathrm{d}\lambda\right\} \tag{95}$$

$$\sigma^1_{13}(x_1,x_2,x_3) = \frac{1}{4\pi(1-v)h^2}\left\{\int_{\lambda=0}^{\lambda=\infty}f_4(\lambda)J_0\left(\frac{\lambda\sqrt{x_1^2+x_2^2}}{h}\right)\mathrm{d}\lambda\right.$$
$$+\frac{1}{2}\left[\int_{\lambda=0}^{\lambda=\infty}(f_5(\lambda)+f_6(\lambda))J_0\left(\frac{\lambda\sqrt{x_1^2+x_2^2}}{h}\right)\mathrm{d}\lambda\right.$$
$$\left.\left.+\frac{x_2^2-x_1^2}{x_1^2+x_2^2}\int_{\lambda=0}^{\lambda=\infty}(f_5(\lambda)-f_6(\lambda))J_2\left(\frac{\lambda\sqrt{x_1^2+x_2^2}}{h}\right)\mathrm{d}\lambda\right]\right\} \tag{96}$$

$$\sigma^1_{22}(x_1,x_2,x_3) = \frac{v}{1-v}\sigma^1_{33}(x_1,x_2,x_3) + \frac{1}{16\pi(1-v)^2h^2}\frac{x_1}{\sqrt{x_1^2+x_2^2}}\left\{(v-1)\frac{x_1^2-3x_2^2}{x_1^2+x_2^2}\right.$$
$$\times\int_{\lambda=0}^{\lambda=\infty}\lambda[f_1(\lambda)-f_2(\lambda)]J_3\left(\frac{\lambda\sqrt{x_1^2+x_2^2}}{h}\right)\mathrm{d}\lambda$$
$$\left.-\int_{\lambda=0}^{\lambda=\infty}\lambda[(1+3v)f_1(\lambda)-(1-v)f_2(\lambda)+4vf_3(\lambda)]J_1\left(\frac{\lambda\sqrt{x_1^2+x_2^2}}{h}\right)\mathrm{d}\lambda\right\} \tag{97}$$

$$\sigma^1_{23}(x_1,x_2,x_3) = \frac{1}{4\pi(1-v)h^2}\frac{-x_1x_2}{x_1^2+x_2^2}\int_{\lambda=0}^{\lambda=\infty}f_7(\lambda)J_2\left(\frac{\lambda\sqrt{x_1^2+x_2^2}}{h}\right)\mathrm{d}\lambda \tag{98}$$

$$\sigma^1_{33}(x_1,x_2,x_3) = \frac{1}{4\pi(1-v)h^2}\frac{-x_1}{\sqrt{x_1^2+x_2^2}}\int_{\lambda=0}^{\lambda=\infty}f_8(\lambda)J_1\left(\frac{\lambda\sqrt{x_1^2+x_2^2}}{h}\right)\mathrm{d}\lambda \tag{99}$$

$$\sigma_{11}^2(x_1,x_2,x_3)=\frac{\nu}{1-\nu}\sigma_{33}^2(x_1,x_2,x_3)+\frac{1}{16\pi(1-\nu)^2h^2}\frac{x_2}{\sqrt{x_1^2+x_2^2}}\left\{(\nu-1)\frac{x_2^2-3x_1^2}{x_1^2+x_2^2}\right.$$

$$\times\int_{\lambda=0}^{\lambda=\infty}\lambda[f_1(\lambda)-f_2(\lambda)]J_3\left(\frac{\lambda\sqrt{x_1^2+x_2^2}}{h}\right)\mathrm{d}\lambda$$

$$\left.-\int_{\lambda=0}^{\lambda=\infty}\lambda[(1+3\nu)f_1(\lambda)-(1-\nu)f_2(\lambda)+4\nu f_3(\lambda)]J_1\left(\frac{\lambda\sqrt{x_1^2+x_2^2}}{h}\right)\mathrm{d}\lambda\right\} \quad (100)$$

$$\sigma_{12}^2(x_1,x_2,x_3)=-\frac{1}{16\pi(1-\nu)h^2}\frac{x_1}{\sqrt{x_1^2+x_2^2}}\left\{\frac{x_1^2-3x_2^2}{x_1^2+x_2^2}\int_{\lambda=0}^{\lambda=\infty}\lambda[f_1(\lambda)-f_2(\lambda)]J_3\left(\frac{\lambda\sqrt{x_1^2+x_2^2}}{h}\right)\mathrm{d}\lambda\right.$$

$$\left.+\int_{\lambda=0}^{\lambda=\infty}\lambda[f_1(\lambda)+f_2(\lambda)+2f_3(\lambda)]J_1\left(\frac{\lambda\sqrt{x_1^2+x_2^2}}{h}\right)\mathrm{d}\lambda\right\} \quad (101)$$

$$\sigma_{13}^2(x_1,x_2,x_3)=\frac{1}{4\pi(1-\nu)h^2}\frac{-x_1x_2}{x_1^2+x_2^2}\int_{\lambda=0}^{\lambda=\infty}f_7(\lambda)J_2\left(\frac{\lambda\sqrt{x_1^2+x_2^2}}{h}\right)\mathrm{d}\lambda \quad (102)$$

$$\sigma_{22}^2(x_1,x_2,x_3)=\frac{\nu}{1-\nu}\sigma_{33}^2(x_1,x_2,x_3)+\frac{1}{16\pi(1-\nu)^2h^2}\frac{x_2}{\sqrt{x_1^2+x_2^2}}\left\{(1-\nu)\frac{x_2^2-3x_1^2}{x_1^2+x_2^2}\right.$$

$$\times\int_{\lambda=0}^{\lambda=\infty}\lambda[f_1(\lambda)-f_2(\lambda)]J_3\left(\frac{\lambda\sqrt{x_1^2+x_2^2}}{h}\right)\mathrm{d}\lambda$$

$$\left.-\int_{\lambda=0}^{\lambda=\infty}\lambda[(3+\nu)f_1(\lambda)+(1-\nu)f_2(\lambda)+4f_3(\lambda)]J_1\left(\frac{\lambda\sqrt{x_1^2+x_2^2}}{h}\right)\mathrm{d}\lambda\right\} \quad (103)$$

$$\sigma_{23}^2(x_1,x_2,x_3)=\frac{1}{4\pi(1-\nu)h^2}\left\{\int_{\lambda=0}^{\lambda=\infty}f_4(\lambda)J_0\left(\frac{\lambda\sqrt{x_1^2+x_2^2}}{h}\right)\mathrm{d}\lambda\right.$$

$$+\frac{1}{2}\left[\int_{\lambda=0}^{\lambda=\infty}(f_5(\lambda)+f_6(\lambda))J_0\left(\frac{\lambda\sqrt{x_1^2+x_2^2}}{h}\right)\mathrm{d}\lambda\right.$$

$$\left.\left.-\frac{x_2^2-x_1^2}{x_1^2+x_2^2}\int_{\lambda=0}^{\lambda=\infty}(f_5(\lambda)-f_6(\lambda))J_2\left(\frac{\lambda\sqrt{x_1^2+x_2^2}}{h}\right)\mathrm{d}\lambda\right]\right\} \quad (104)$$

$$\sigma_{33}^2(x_1,x_2,x_3)=\frac{1}{4\pi(1-\nu)h^2}\frac{-x_2}{\sqrt{x_1^2+x_2^2}}\int_{\lambda=0}^{\lambda=\infty}f_8(\lambda)J_1\left(\frac{\lambda\sqrt{x_1^2+x_2^2}}{h}\right)\mathrm{d}\lambda \quad (105)$$

$$\sigma_{11}^3(x_1,x_2,x_3)=\frac{\nu}{1-\nu}\sigma_{33}^3(x_1,x_2,x_3)+\frac{1}{8\pi(1-\nu)^2h^2}\left\{(1+\nu)\int_{\lambda=0}^{\lambda=\infty}\left[\lambda f_9(\lambda)J_0\left(\frac{\lambda\sqrt{x_1^2+x_2^2}}{h}\right)\right.\right.$$

$$\left.-12(1-\nu)^2(2\chi-1)\frac{\mathrm{e}^{-\lambda}}{\lambda}\right]\mathrm{d}\lambda$$

$$\left.+(1-\nu)\frac{x_2^2-x_1^2}{x_1^2+x_2^2}\int_{\lambda=0}^{\lambda=\infty}\lambda f_9(\lambda)J_2\left(\frac{\lambda\sqrt{x_1^2+x_2^2}}{h}\right)\mathrm{d}\lambda\right\} \quad (106)$$

$$\sigma_{12}^{3}(x_1,x_2,x_3) = -\frac{1}{4\pi(1-\nu)h^2}\frac{x_1x_2}{x_1^2+x_2^2}\int_{\lambda=0}^{\lambda=\infty}\lambda f_9(\lambda)J_2\left(\frac{\lambda\sqrt{x_1^2+x_2^2}}{h}\right)\mathrm{d}\lambda \tag{107}$$

$$\sigma_{13}^{3}(x_1,x_2,x_3) = \frac{1}{4\pi(1-\nu)h^2}\frac{x_1}{\sqrt{x_1^2+x_2^2}}\int_{\lambda=0}^{\lambda=\infty}f_{10}(\lambda)J_1\left(\frac{\lambda\sqrt{x_1^2+x_2^2}}{h}\right)\mathrm{d}\lambda \tag{108}$$

$$\begin{aligned}\sigma_{22}^{3}(x_1,x_2,x_3) = \frac{\nu}{1-\nu}\sigma_{33}^{3}(x_1,x_2,x_3) + \frac{1}{8\pi(1-\nu)^2h^2}\Bigg\{(1+\nu)\int_{\lambda=0}^{\lambda=\infty}\Bigg[\lambda f_9(\lambda)J_0\left(\frac{\lambda\sqrt{x_1^2+x_2^2}}{h}\right)\\ -12(1-\nu)^2(2\chi-1)\frac{\mathrm{e}^{-\lambda}}{\lambda}\Bigg]\mathrm{d}\lambda\\ +(1-\nu)\frac{x_1^2-x_2^2}{x_1^2+x_2^2}\int_{\lambda=0}^{\lambda=\infty}\lambda f_9(\lambda)J_2\left(\frac{\lambda\sqrt{x_1^2+x_2^2}}{h}\right)\mathrm{d}\lambda\Bigg\}\end{aligned} \tag{109}$$

$$\sigma_{23}^{3}(x_1,x_2,x_3) = \frac{1}{4\pi(1-\nu)h^2}\frac{x_2}{\sqrt{x_1^2+x_2^2}}\int_{\lambda=0}^{\lambda=\infty}f_{10}(\lambda)J_1\left(\frac{\lambda\sqrt{x_1^2+x_2^2}}{h}\right)\mathrm{d}\lambda \tag{110}$$

$$\sigma_{33}^{3}(x_1,x_2,x_3) = \frac{1}{4\pi(1-\nu)h^2}\int_{\lambda=0}^{\lambda=\infty}f_{11}(\lambda)J_0\left(\frac{\lambda\sqrt{x_1^2+x_2^2}}{h}\right)\mathrm{d}\lambda \tag{111}$$

$$\begin{aligned}u_1^{1}(x_1,x_2,x_3) = \frac{1+\nu}{4\pi(1-\nu)h}\frac{1}{E}\Bigg\{\int_{\lambda=0}^{\lambda=\infty}\Bigg\{[f_3(\lambda)+\tfrac{1}{2}(f_1(\lambda)+f_2(\lambda))]J_0\left(\frac{\lambda\sqrt{x_1^2+x_2^2}}{h}\right)\\ -(\nu-1)[6(1-\nu)(\chi+\psi-2\chi\psi)+2(2\nu-3)]\frac{\mathrm{e}^{-\lambda}}{\lambda}\Bigg\}\mathrm{d}\lambda\\ +\frac{1}{2}\frac{x_2^2-x_1^2}{x_1^2+x_2^2}\int_{\lambda=0}^{\lambda=\infty}(f_1(\lambda)-f_2(\lambda))J_2\left(\frac{\lambda\sqrt{x_1^2+x_2^2}}{h}\right)\mathrm{d}\lambda\Bigg\}\end{aligned} \tag{112}$$

$$u_2^{1}(x_1,x_2,x_3) = \frac{1+\nu}{4\pi(1-\nu)h}\frac{1}{E}\frac{-x_1x_2}{x_1^2+x_2^2}\int_{\lambda=0}^{\lambda=\infty}f_{12}(\lambda)J_2\left(\frac{\lambda\sqrt{x_1^2+x_2^2}}{h}\right)\mathrm{d}\lambda \tag{113}$$

$$\begin{aligned}u_3^{1}(x_1,x_2,x_3) = \frac{1+\nu}{4\pi(1-\nu)h}\frac{1}{E}\frac{-x_1}{\sqrt{x_1^2+x_2^2}}\int_{\lambda=0}^{\lambda=\infty}\Bigg\{f_{13}(\lambda)J_1\left(\frac{\lambda\sqrt{x_1^2+x_2^2}}{h}\right)\\ -6(1-\nu)^2\frac{\sqrt{x_1^2+x_2^2}}{h}(2\psi-1)\frac{\mathrm{e}^{-\lambda}}{\lambda}\Bigg\}\mathrm{d}\lambda\end{aligned} \tag{114}$$

$$u_1^{2}(x_1,x_2,x_3) = \frac{1+\nu}{4\pi(1-\nu)h}\frac{1}{E}\frac{-x_1x_2}{x_1^2+x_2^2}\int_{\lambda=0}^{\lambda=\infty}f_{12}(\lambda)J_2\left(\frac{\lambda\sqrt{x_1^2+x_2^2}}{h}\right)\mathrm{d}\lambda \tag{115}$$

$$\begin{aligned}u_2^{2}(x_1,x_2,x_3) = \frac{1+\nu}{4\pi(1-\nu)h}\frac{1}{E}\Bigg\{\int_{\lambda=0}^{\lambda=\infty}\Bigg\{[f_3(\lambda)+\tfrac{1}{2}(f_1(\lambda)+f_2(\lambda))]J_0\left(\frac{\lambda\sqrt{x_1^2+x_2^2}}{h}\right)\\ -(\nu-1)[6(1-\nu)(\chi+\psi-2\chi\psi)+2(2\nu-3)]\frac{\mathrm{e}^{-\lambda}}{\lambda}\Bigg\}\mathrm{d}\lambda\\ -\frac{1}{2}\frac{x_2^2-x_1^2}{x_1^2+x_2^2}\int_{\lambda=0}^{\lambda=\infty}(f_1(\lambda)-f_2(\lambda))J_2\left(\frac{\lambda\sqrt{x_1^2+x_2^2}}{h}\right)\mathrm{d}\lambda\Bigg\}\end{aligned} \tag{116}$$

$$u_3^2(x_1,x_2,x_3)=\frac{1+\nu}{4\pi(1-\nu)h}\frac{1}{E}\frac{-x_2}{\sqrt{x_1^2+x_2^2}}\int_{\lambda=0}^{\lambda=\infty}\left\{f_{13}(\lambda)J_1\left(\frac{\lambda\sqrt{x_1^2+x_2^2}}{h}\right)\right.$$
$$\left.-6(1-\nu)^2\frac{\sqrt{x_1^2+x_2^2}}{h}(2\psi-1)\frac{e^{-\lambda}}{\lambda}\right\}d\lambda \tag{117}$$

$$u_1^3(x_1,x_2,x_3)=\frac{1+\nu}{4\pi(1-\nu)h}\frac{1}{E}\frac{x_1}{\sqrt{x_1^2+x_2^2}}\int_{\lambda=0}^{\lambda=\infty}\left\{f_9(\lambda)J_1\left(\frac{\lambda\sqrt{x_1^2+x_2^2}}{h}\right)\right.$$
$$\left.-6(1-\nu)^2\frac{\sqrt{x_1^2+x_2^2}}{h}(2\chi-1)\frac{e^{-\lambda}}{\lambda}\right\}d\lambda \tag{118}$$

$$u_2^3(x_1,x_2,x_3)=\frac{1+\nu}{4\pi(1-\nu)h}\frac{1}{E}\frac{x_2}{\sqrt{x_1^2+x_2^2}}\int_{\lambda=0}^{\lambda=\infty}\left\{f_9(\lambda)J_1\left(\frac{\lambda\sqrt{x_1^2+x_2^2}}{h}\right)\right.$$
$$\left.-6(1-\nu)^2\frac{\sqrt{x_1^2+x_2^2}}{h}(2\chi-1)\frac{e^{-\lambda}}{\lambda}\right\}d\lambda \tag{119}$$

$$u_3^3(x_1,x_2,x_3)=\frac{1+\nu}{4\pi(1-\nu)h}\frac{1}{E}\int_{\lambda=0}^{\lambda=\infty}\left\{f_{14}(\lambda)J_0\left(\frac{\lambda\sqrt{x_1^2+x_2^2}}{h}\right)-\frac{24(1-\nu)^2}{\lambda^3}\right.$$
$$\left.-\left[12\nu(1-\nu)(\chi+\psi-\chi^2-\psi^2)+\frac{24}{5}(1-\nu)^2-6(1-\nu)^2\frac{x_1^2+x_2^2}{h}\right]\frac{e^{-\lambda}}{\lambda}\right\}d\lambda \tag{120}$$

where the superscripts 1, 2, 3 indicate the direction of the unit load and $\chi = x_3/h$, $\psi = H/h$.

For the sake of brevity, expressions for $f_*(\lambda,\chi,\psi)$ defined in (94)–(120) are functions of λ, χ, ψ, E and ν, and they should be taken as $f_*^*(\lambda,\chi,\psi,E,\nu)$. They are given by

$$f_1(\lambda)=\frac{1}{\sinh^2(\lambda)-\lambda^2}\left\{\lambda^3\chi(\psi-1)\cosh[\lambda(\chi-\psi)]+\frac{\lambda^2}{2}[(4\nu-3)(1+\chi-\psi)\sinh[\lambda(\chi-\psi)]\right.$$
$$+(1-\chi)(1-\psi)\sinh[\lambda(\chi+\psi)]+\chi\psi\sinh[\lambda(2-\chi-\psi)]]$$
$$-\frac{\lambda}{4}[(2(8\nu^2-12\nu+5)+\chi-\psi)\cosh[\lambda(\chi-\psi)]+(3-4\nu)(2-\chi-\psi)\cosh[\lambda(\chi+\psi)]$$
$$+(3-4\nu)(\chi+\psi)\cosh[\lambda(2-\chi-\psi)]+(\psi-\chi)\cosh[\lambda(2+\chi-\psi)]]$$
$$+\frac{1}{4}[(8\nu^2-8\nu+1)\sinh[\lambda(\chi+\psi)]+(8\nu^2-8\nu+1)\sinh[\lambda(2-\chi-\psi)]$$
$$\left.+\sinh[\lambda(\chi-\psi)]-\sinh[\lambda(2+\chi-\psi)]]\right\}$$
$$+\{-\lambda(\chi-\psi)\cosh[\lambda(\chi-\psi)]+\sinh[\lambda(\chi-\psi)]\}\mathscr{H}(\chi-\psi) \tag{121}$$

$$f_2(\lambda)=\frac{1}{\sinh^2(\lambda)-\lambda^2}\left[-4(1-\nu)\lambda^2\frac{\cosh(\lambda\chi)\cosh[\lambda(1-\psi)]}{\sinh(\lambda)}\right] \tag{122}$$

$$f_3(\lambda)=\frac{1}{\sinh^2(\lambda)-\lambda^2}\{(1-\nu)[\sinh[\lambda(\chi+\psi)]-\sinh[\lambda(\chi-\psi)]+\sinh[\lambda(2-\chi-\psi)]$$
$$+\sinh[\lambda(2+\chi-\psi)]]\}+\{-4(1-\nu)\sinh[\lambda(\chi-\psi)]\}\mathscr{H}(\chi-\psi) \tag{123}$$

$$f_4(\lambda)=\frac{1}{\sinh^2(\lambda)-\lambda^2}\left\{(1-\nu)\frac{\lambda}{2}[\cosh[\lambda(\chi+\psi)]-\cosh[\lambda(\chi-\psi)]-\cosh[\lambda(2-\chi-\psi)]\right.$$
$$\left.+\cosh[\lambda(2+\chi-\psi)]]\right\}+\{-\lambda 2(1-\nu)\cosh[\lambda(\chi-\psi)]\}\mathscr{H}(\chi-\psi) \tag{124}$$

$$f_5(\lambda)=\frac{1}{\sinh^2(\lambda)-\lambda^2}\left\{\lambda^4\chi(\psi-1)\sinh[\lambda(\chi-\psi)]+\frac{\lambda^3}{2}[(1-\chi)(1-\psi)\cosh[\lambda(\chi+\psi)]\right.$$
$$+((4\nu-3)\chi+\psi-1)\cosh[\lambda(\chi-\psi)]-\chi\psi\cosh[\lambda(2-\chi-\psi)]]$$
$$+\frac{\lambda^2}{4}[((3-4\nu)\chi+4(\nu-1)+\psi)\sinh[\lambda(\chi+\psi)]+(4(\nu-1)-\chi+\psi)\sinh[\lambda(\chi-\psi)]$$
$$\left.+((3-4\nu)\chi+\psi)\sinh[\lambda(2-\chi-\psi)]+(\chi-\psi)\sinh[\lambda(2+\chi-\psi)]]\right\}$$
$$+\{\lambda^2(\psi-\chi)\sinh[\lambda(\chi-\psi)]\}\mathscr{H}(\chi-\psi) \tag{125}$$

$$f_6(\lambda)=\frac{1}{\sinh^2(\lambda)-\lambda^2}\left\{-2(1-\nu)\lambda^3\frac{\sinh(\lambda\chi)\cosh[\lambda(1-\psi)]}{\sinh(\lambda)}\right\} \tag{126}$$

$$f_7(\lambda)=\frac{1}{\sinh^2(\lambda)-\lambda^2}\left\{\lambda^4\chi(\psi-1)\sinh[\lambda(\chi-\psi)]+\frac{\lambda^3}{2}[(1-\chi)(1-\psi)\cosh[\lambda(\chi+\psi)]\right.$$
$$+((4\nu-3)\chi+\psi-1)\cosh[\lambda(\chi-\psi)]-\chi\psi\cosh[\lambda(2-\chi-\psi)]]$$
$$+\frac{\lambda^2}{4}[((3-4\nu)\chi+4(\nu-1)+\psi)\sinh[\lambda(\chi+\psi)]+(4(\nu-1)-\chi+\psi)\sinh[\lambda(\chi-\psi)]$$
$$+((3-4\nu)\chi+\psi)\sinh[\lambda(2-\chi-\psi)]+(\chi-\psi)\sinh[\lambda(2+\chi-\psi)]]$$
$$\left.+2(1-\nu)\lambda^3\frac{\sinh(\lambda\chi)\cosh[\lambda(1-\psi)]}{\sinh(\lambda)}\right\}$$
$$+\{\lambda^2(\psi-\chi)\sinh[\lambda(\chi-\psi)]\}\mathscr{H}(\chi-\psi) \tag{127}$$

$$f_8(\lambda)=\frac{1}{\sinh^2(\lambda)-\lambda^2}\left\{\lambda^4\chi(1-\psi)\cosh[\lambda(\chi-\psi)]-\frac{\lambda^3}{2}[(1-\chi)(1-\psi)\sinh[\lambda(\chi+\psi)]\right.$$
$$+((4\nu-3)\chi-\psi+1)\sinh[\lambda(\chi-\psi)]+\chi\psi\sinh[\lambda(2-\chi-\psi)]]$$
$$+\frac{\lambda^2}{4}[((4\nu-3)\chi+2(1-2\nu)+\psi)\cosh[\lambda(\chi+\psi)]+(2(2\nu-1)+\chi-\psi)\cosh[\lambda(\chi-\psi)]$$
$$+((3-4\nu)\chi-\psi)\cosh[\lambda(2-\chi-\psi)]+(\psi-\chi)\cosh[\lambda(2+\chi-\psi)]]$$
$$\left.-(2\nu-1)\frac{\lambda}{4}[\sinh[\lambda(\chi+\psi)]+\sinh[\lambda(\chi-\psi)]+\sinh[\lambda(2-\chi-\psi)]-\sinh[\lambda(2+\chi-\psi)]]\right\}$$
$$+\{\lambda^2(\chi-\psi)\cosh[\lambda(\chi-\psi)]-\lambda(2\nu-1)\sinh[\lambda(\chi-\psi)]\}\mathscr{H}(\chi-\psi) \tag{128}$$

$$f_9(\lambda)=\frac{1}{\sinh^2(\lambda)-\lambda^2}\Big\{\lambda^3\chi(\psi-1)\sinh[\lambda(\chi-\psi)]-\frac{\lambda^2}{2}[(1-\chi)(1-\psi)\cosh[\lambda(\chi+\psi)]$$
$$+(4\nu-3)(\chi+\psi-1)\cosh[\lambda(\chi-\psi)]-\chi\psi\cosh[\lambda(2-\chi-\psi)]]$$
$$+\frac{\lambda}{4}[(4\nu-3)(\psi-\chi)\sinh[\lambda(\chi+\psi)]+(8(2\nu-1)(\nu-1)-\chi+\psi)\sinh[\lambda(\chi-\psi)]$$
$$+(4\nu-3)(\psi-\chi)\sinh[\lambda(2-\chi-\psi)]+(\chi-\psi)\sinh[\lambda(2+\chi-\psi)]]$$
$$+(2\nu-1)(\nu-1)[\cosh[\lambda(\chi+\psi)]-\cosh[\lambda(2-\chi-\psi)]]\Big\}$$
$$+\{\lambda(\psi-\chi)\sinh[\lambda(\chi-\psi)]\}\mathscr{H}(\chi-\psi) \tag{129}$$

$$f_{10}(\lambda)=\frac{1}{\sinh^2(\lambda)-\lambda^2}\Big\{\lambda^4\chi(\psi-1)\cosh[\lambda(\chi-\psi)]-\frac{\lambda^3}{2}[(1-\chi)(1-\psi)\sinh[\lambda(\chi+\psi)]$$
$$+((4\nu-3)\chi-\psi+1)\sinh[\lambda(\chi-\psi)]+\chi\psi\sinh[\lambda(2-\chi-\psi)]]$$
$$-\frac{\lambda^2}{4}[((4\nu-3)\chi+2(1-2\nu)+\psi)\cosh[\lambda(\chi+\psi)]+(2(2\nu-1)+\chi-\psi)\cosh[\lambda(\chi-\psi)]$$
$$+((3-4\nu)\chi-\psi)\cosh[\lambda(2-\chi-\psi)]+(\psi-\chi)\cosh[\lambda(2+\chi-\psi)]]$$
$$-(2\nu-1)\frac{\lambda}{4}[\sinh[\lambda(\chi+\psi)]+\sinh[\lambda(\chi-\psi)]$$
$$+\sinh[\lambda(2-\chi-\psi)]-\sinh[\lambda(2+\chi-\psi)]]\Big\}$$
$$+\{-\lambda^2(\chi-\psi)\cosh[\lambda(\chi-\psi)]-\lambda(2\nu-1)\sinh[\lambda(\chi-\psi)]\}\mathscr{H}(\chi-\psi) \tag{130}$$

$$f_{11}(\lambda)=\frac{1}{\sinh^2(\lambda)-\lambda^2}\Big\{\lambda^4\chi(1-\psi)\sinh[\lambda(\chi-\psi)]+\frac{\lambda^3}{2}[(1-\chi)(1-\psi)\cosh[\lambda(\chi+\psi)]$$
$$+((4\nu-3)\chi+\psi-1)\cosh[\lambda(\chi-\psi)]-\chi\psi\cosh[\lambda(2-\chi-\psi)]]$$
$$+\frac{\lambda^2}{4}[((4\nu-3)\chi+4(1-\nu)-\psi)\sinh[\lambda(\chi+\psi)]+(4(1-\nu)+\chi-\psi)\sinh[\lambda(\chi-\psi)]$$
$$+((4\nu-3)\chi-\psi)\sinh[\lambda(2-\chi-\psi)]+(\psi-\chi)\sinh[\lambda(2+\chi-\psi)]]$$
$$-(1-\nu)\frac{\lambda}{2}[-\cosh[\lambda(\chi+\psi)]+\cosh[\lambda(\chi-\psi)]$$
$$+\cosh[\lambda(2-\chi-\psi)]-\cosh[\lambda(2+\chi-\psi)]]\Big\}$$
$$+\{\lambda^2(\chi-\psi)\sinh[\lambda(\chi-\psi)]-\lambda2(1-\nu)\cosh[\lambda(\chi-\psi)]\}\mathscr{H}(\chi-\psi) \tag{131}$$

$$f_{12}(\lambda)=\frac{1}{\sinh^2(\lambda)-\lambda^2}\Big\{\lambda^3\chi(\psi-1)\cosh[\lambda(\chi-\psi)]+\frac{\lambda^2}{2}[((2\nu-1)+\chi\psi-\chi-\psi)\sinh[\lambda(\chi+\psi)]$$
$$+((2\nu-1)+(3-4\nu)(\psi-\chi))\sinh[\lambda(\chi-\psi)]$$
$$+(2(\nu-1)+\chi\psi)\sinh[\lambda(2-\chi-\psi)]+2(\nu-1)\sinh[\lambda(2+\chi-\psi)]]$$
$$-\frac{\lambda}{4}[(2(8\nu^2-12\nu+5)+\chi-\psi)\cosh[\lambda(\chi-\psi)]+(3-4\nu)(2-\chi-\psi)\cosh[\lambda(\chi+\psi)]]$$
$$+(3-4\nu)(\chi+\psi)\cosh[\lambda(2-\chi-\psi)]+(\psi-\chi)\cosh[\lambda(2+\chi-\psi)]]$$
$$+\frac{1}{4}[(8\nu^2-8\nu+1)\sinh[\lambda(\chi+\psi)]+(8\nu^2-8\nu+1)\sinh[\lambda(2-\chi-\psi)]$$
$$+\sinh[\lambda(\chi-\psi)]-\sinh[\lambda(2+\chi-\psi)]]$$
$$+4(1-\nu)\lambda^2\frac{\cosh^2(\lambda)\cosh(\lambda\chi)}{\sinh(\lambda)}\cosh[\lambda(1-\psi)]\Big\}$$
$$+\{-\lambda(\chi-\psi)\cosh[\lambda(\chi-\psi)]+\sinh[\lambda(\chi-\psi)]\}\mathscr{H}(\chi-\psi) \tag{132}$$

$$f_{13}(\lambda)=\frac{1}{\sinh^2(\lambda)-\lambda^2}\Big\{\lambda^3\chi(1-\psi)\sinh[\lambda(\chi-\psi)]-\frac{\lambda^2}{2}[(1-\chi)(1-\psi)\cosh[\lambda(\chi+\psi)]$$
$$+(3-4\nu)(1-\chi-\psi)\cosh[\lambda(\chi-\psi)]-\chi\psi\cosh[\lambda(2-\chi-\psi)]]$$
$$-\frac{\lambda}{4}[(3-4\nu)(\chi-\psi)\sinh[\lambda(\chi+\psi)]+(8(2\nu-1)(\nu-1)-\chi+\psi)\sinh[\lambda(\chi-\psi)]$$
$$+(3-4\nu)(\chi-\psi)\sinh[\lambda(2-\chi-\psi)]+(\chi-\psi)\sinh[\lambda(2+\chi-\psi)]]$$
$$+(2\nu-1)(\nu-1)[\cosh[\lambda(\chi+\psi)]-\cosh[\lambda(2-\chi-\psi)]]\Big\}$$
$$+\{-\lambda(\psi-\chi)\sinh[\lambda(\chi-\psi)]\}\mathscr{H}(\chi-\psi) \tag{133}$$

$$f_{14}(\lambda)=\frac{1}{\sinh^2(\lambda)-\lambda^2}\Big\{\lambda^3\chi(1-\psi)\cosh[\lambda(\chi-\psi)]+\frac{\lambda^2}{2}[(4\nu-3)(1+\chi-\psi)\sinh[\lambda(\chi-\psi)]$$
$$+(1-\chi)(1-\psi)\sinh[\lambda(\chi+\psi)]+\chi\psi\sinh[\lambda(2-\chi-\psi)]]$$
$$+\frac{\lambda}{4}[(2(8\nu^2-12\nu+5)+\chi-\psi)\cosh[\lambda(\chi-\psi)]+(3-4\nu)(2-\chi-\psi)\cosh[\lambda(\chi+\psi)]$$
$$+(3-4\nu)(\chi+\psi)\cosh[\lambda(2-\chi-\psi)]+(\psi-\chi)\cosh[\lambda(2+\chi-\psi)]]$$
$$+\frac{1}{4}[(8\nu^2-12\nu+5)\sinh[\lambda(\chi+\psi)]+(8\nu^2-12\nu+5)\sinh[\lambda(2-\chi-\psi)]$$
$$+(4\nu-3)\sinh[\lambda(\chi-\psi)]-(4\nu-3)\sinh[\lambda(2+\chi-\psi)]]\Big\}$$
$$+\{\lambda(\chi-\psi)\cosh[\lambda(\chi-\psi)]+(4\nu-3)\sinh[\lambda(\chi-\psi)]\}\mathscr{H}(\chi-\psi) \tag{134}$$

where $\mathscr{H}(\chi - \psi)$ represents the Heaviside function, given by

$$\mathscr{H}(\chi - \psi) = \begin{cases} 1 & \text{for } \chi \geqslant \psi \\ 0 & \text{for } \chi < \psi \end{cases} \tag{135}$$

APPENDIX II

The expressions for the analytical integration $G(\mu, a, b, c)$, defined in (73), with the structure

$$G(\mu, a, b, c) = \int_0^\infty \lambda^a \mathrm{e}^{-c\lambda} J_\mu(b\lambda)\,\mathrm{d}\lambda \quad \forall c > 0 \tag{136}$$

are listed below

$$G(0,0,b,c) = \frac{1}{R} \tag{137}$$

$$G(0,1,b,c) = \frac{c}{R^3} \tag{138}$$

$$G(0,2,b,c) = -\frac{1}{R^3}\left(1 - \frac{3c^2}{R^2}\right) \tag{139}$$

$$G(0,3,b,c) = -\frac{3c}{R^5}\left(3 - \frac{5c^2}{R^2}\right) \tag{140}$$

$$G(0,4,b,c) = \frac{3}{R^5}\left(3 - \frac{30c^2}{R^2} + \frac{35c^4}{R^4}\right) \tag{141}$$

$$G(1,0,b,c) = \frac{b}{R(R+c)} \tag{142}$$

$$G(1,1,b,c) = \frac{b}{R^3} \tag{143}$$

$$G(1,2,b,c) = \frac{3bc}{R^5} \tag{144}$$

$$G(1,3,b,c) = -\frac{3b}{R^5}\left(1 - \frac{5c^2}{R^2}\right) \tag{145}$$

$$G(1,4,b,c) = -\frac{15bc}{R^7}\left(3 - \frac{7c^2}{R^2}\right) \tag{146}$$

$$G(2,0,b,c) = \frac{b^2}{R(R+c)^2} \tag{147}$$

$$G(2,1,b,c) = \frac{b^2}{R^2(R+c)^2}\left(2 + \frac{c}{R}\right) \tag{148}$$

$$G(2,2,b,c) = \frac{3b^2}{R^5} \tag{149}$$

$$G(2,3,b,c) = \frac{15b^2c}{R^7} \tag{150}$$

$$G(2,4,b,c) = \frac{15b^2}{R^7}\left(6 - \frac{7b^2}{R^2}\right) \tag{151}$$

$$G(3,0,b,c) = \frac{b^3}{R(R+c)^3} \tag{152}$$

$$G(3,1,b,c) = \frac{b^3}{R^2(R+c)^3}\left(3 + \frac{c}{R}\right) \tag{153}$$

$$G(3,2,b,c) = \frac{b^3}{R^3(R+c)^3}\left(8 + \frac{9c}{R} + \frac{3c^2}{R^2}\right) \tag{154}$$

$$G(3,3,b,c) = \frac{15b^3}{R^7} \tag{155}$$

$$G(3,4,b,c) = \frac{105b^3c}{R^9} \tag{156}$$

where $R = \sqrt{b^2 + c^2}$.

REFERENCES

1. W. Thompson (Lord Kelvin), 'On the equations of equilibrium of an elastic solid', *Cambridge and Dublin Math. J.*, **3**, 87–89 (1848).
2. T. A. Cruse, 'Numerical solutions in three-dimensional elastostatics', *Int. J. Solids Struct.*, **5**, 1259–1274 (1969).
3. F. J. Rizzo, 'An integral equation approach to boundary value problems of classical elastostics', *Quart. Appl. Math.*, **25**, 83–95 (1967).
4. E. Melan, 'Der Spannungszustand der durch eine Einzelkraft in innenn Beanspruchten Halbscheibe', *Z. Angew Math. Mech.*, **12**, 343–346 (1932).
5. R. D. Mindlin, 'Force at a point in the interior of a semi-infinite solid', *Physics*, **7**, 195–202 (1936).
6. J. C. F. Telles and C. A. Brebbia, 'Boundary element solution for half-plane problems'. *Int. J. Solids Struct.*, **17**, 1149–1158 (1981).
7. R. Butterfield and P. K. Banerjee, 'The problem of pile cap, pile group interaction', *Géotechnique*, **21**, 135 141 (1971).
8. F. G. Benitez and A. J. Rosakis, 'Three dimensional elastostatics of a layer and a layered medium', SM85-21, Division of Engineering and Applied Sciences, California Inst. of Technology, Pasadena, CA, 1985.
9. F. G. Benitez and A. J. Rosakis, 'Three dimensional elastostatics of a layer and a layered medium', *J. Elasticity*, **18**, 3–50 (1987).
10. O. D. Kellog, *Foundations of Potential Theory*, Dover, New York, 1953.
11. I. S. Sokolnikoff, *Mathematical Theory of Elasticity*, 2nd ed., McGraw-Hill, New York, 1952.
12. F. G. Benitez and A. J. Rosakis, 'A modified boundary integral formulation for the study of 3-D crack problems in plates', in *Analytical, Numerical and Experimental Aspects of Three Dimensional Fracture Processes*, ASME AMD-91, 1988, pp. 99–112.
13. M. J. Turteltaub and E. Sternberg, 'On concentrated loads and Green's functions in elastostatics', *Arch. Rat. Mech. Anal.*, **29**, 193–240 (1968).
14. F. Hartmann, 'Computing the C-matrix in non-smooth boundary points', in C. A. Brebbia (ed.), *New Developments in Boundary Element Methods*, CML, Southampton, 1980, pp. 367–379.
15. M. Stippes and F. J. Rizzo, 'A note on the body force integral of classical elastostatics', *Z. Angew. Math. Phys.*, **28**, 339 341 (1977).
16. T. C. Cruse, private communication, 1989.
17. C. A. Brebbia, *The Boundary Element Method for Engineers*, Pentech Press, Plymouth, 1978.